Humboldt-Universität zu Berlin
MATHEMATISCH-NATURWISSENSCHAFTLICHE FAKULTÄT I
INSTITUT FÜR BIOLOGIE

MASTERARBEIT

ZUM ERWERB DES AKADEMISCHEN GRADES
MASTER OF SCIENCE

„Computergestützte Modellierung und Analyse des mehrfach verzweigten HOG-Signalweges der Bäckerhefe “

„Computational Modelling and Analysis of the Baker’s Yeast Multi-Branch HOG Pathway“

vorgelegt von
Gady Goldsobel
angefertigt in der Arbeitsgruppe Theoretische Biophysik
am Institut für Biologie
Berlin, im Dezember 2010

Eine kurze Zusammenfassung in deutscher Sprache

Die osmotische Stress-Reaktion und der mit ihr verbundene HOG-Signalweg (High Osmolarity Glycerol) ist eines der am intensivsten untersuchten Systeme in der Bäckerhefe Saccharomyces cerevisiae.
Die in extrem rauen Umgebungen und unter harten Bedingungen (wie hoher Osmolarität) lebenden Hefezellen, zeigen eine enorme Fähigkeit, sich diesen Bedingungen anpassen. Die Evolution hat den HOG-Signalweg optimiert, sodass die Zellen in der Lage sind, innerhalb weniger Minuten zu reagieren, und einen regelmäßigen Zellstoffwechsel und Zellwachstum unter Druck nachhaltig aufrechtzuerhalten. Fasziniert von der erstaunlichen Überlebensfähigkeit von Hefezellen, begannen Forscher, Saccharomyces cerevisiae vor mehr als zwei Jahrzehnten zu untersuchen, um die Biologie ihrer osmotischen Stress-Reaktion und die dafür verantwortlichen Mechanismen zu enträtseln.
Neben der Identifizierung der wichtigsten Akteure im Signalweg und der Aufklärung ihrer biochemischen Rolle in zahlreichen Experimenten, haben Systembiologen begonnen, mathematische Modelle dieses Weges zu entwickeln, um Bedingungen, die nicht im Labor reproduziert werden können, zu simulieren. Auf diese Weise hoffen Systembiologen zu einem noch besseren Verständnis des Signalweges zu gelangen. Solche Modelle können Forschern helfen, adäquate Experimente zu entwerfen, um ihre theoretischen Hypothesen zu überprüfen. Da der HOG-Signalweg mit anderen Signalwegen in anderen Organismen verwandt ist, ist die Hoffnung, dass eine klarere Interpretation der Prozesse eine bessere Sicht auf andere Systeme und ein besseres Verständnis der zugrunde liegenden Prinzipien und Mechanismen biologischer Systeme ermöglichen wird.
Diese Arbeit beinhaltet die Schaffung eines solchen mathematischen Modells. Das Modell stützt sich zum Teil auf bekannte Modelle des HOG-Signalwegs, wie die von Klipp et al (2005) und Zhike et al (2009). Die wichtigsten Ziele dieser Arbeit waren, das Modell unter verschiedenen Graden vom osmotischen Stress zu untersuchen und die Integration der beiden Zweige der osmotischen Stress-Reaktion, nämlich des Sho1 Zweiges und des Sln1 Zweiges, zu erforschen. Die Daten über das Verhalten der Hefe unter solchen Bedingungen wurden in Experimenten von Macia et al (2009) gewonnen. Um als zuverlässig zu gelten, soll das Modell den Ergebnissen dieser Experimente entsprechen. Seine Gültigkeit ist auch durch den Nachweis, dass andere Eigenschaften des Modells, wie biophysikalische Veränderungen, im Einklang mit anderen experimentellen Daten sind, und dass das Modell robust gegenüber Störungen von den ursprünglichen Spezieskonzentrationen ist. Informationsübertragung im System wurde mathematisch untersucht und eine Sensitivitätsanalyse durchgeführt, um die Rolle und Wichtigkeit der Spezies und Parameter des Systems genauer zu untersuchen. Darüber hinaus stellt diese Arbeit die Hypothese der Existenz eines Feed-forward-Mechanismus im System auf und beschreibt ein Szenario, in dem ein solcher Mechanismus von Bedeutung sein könnte. Als ein Beispiel für eine Implementierung jenes hypothetischen Feed-forward-Mechanismus ist die Regulation der Hot1 Expression durch Skn7 eingeführt. Skn7 war bisher nur für seine Rollen in anderen Signalwegen bekannt. Seine Beteiligung an dem HOG-Signalweg wurde bisher nie gezeigt. Diese Arbeit ist rein theoretisch und als solche könnte sie als eine Plattform für weitere Untersuchungen und Vorhersagen über das Verhalten der Hefe unter verschiedenen Umgebungsbedingungen eingesetzt werden. Solche vorhersagen können später in Experimenten bestätigt werden und ein neues Licht auf die Hefe-Osmoadaptation und die Reaktion auf osmotischen Stress werfen.

Contents

1 **Introduction** *4*
2 **The Model** *6*
2.1 Model Graphical Presentation *6*
2.2 Biochemical and Mathematical Principles *7*
2.2.1 Model Inputs *7*
2.2.2 The Sln1 Branch *8*
2.2.2.1 Phosphorelay *9*
2.2.2.2 Ssk2-Pbs2-Pbs2p *9*
2.2.2.3 Ypd1 as a Junction *9*
2.2.3 The Sho1 Branch *10*
2.2.4 Skn7 and Hot1 *10*
2.2.5 Pbs2 *11*
2.2.6 Hog1 *12*
2.2.7 Glycerol Production and Outflow *12*
2.2.8 Biophysical Changes *14*
2.2.9 Initial conditions and Parameters *14*
2.2.10 Sensitivity Analysis *14*
2.2.11 Normalization *15*
3 **Results** *15*
3.1 Modelling Experimental Data *15*
3.1.1 ΔSsk2/ΔSsk22 *16*
3.1.2 ΔSte11 Strain *19*
3.1.3 Wild Type simulation *20*
3.2 Species' Properties and Kinetics *21*
3.2.1 Biophysical Changes *21*
3.2.1.1 Glycerol Intracellular Concentration *21*
3.2.1.2 Cell Volume *22*
3.2.2 Fps1 Mutant *24*
3.2.3 mRNA Species *25*
3.3 The Feed-Forward Mechanism *26*
3.3.1 Hot1 mRNA Regulation as an Example of a Hypothetic Feet-Forward Mechanism *26*
3.3.2 Effects of Skn7 on the Osmoadaptation *30*
3.4 Integration of Sln1 and Sho1 Branches *31*
3.5 Information Flow in the System *36*
3.5.1 Information Transmission in the Wild Type *37*
3.5.1.1 Phosphorelay Module *38*
3.5.1.2 Hot1 Expression Module *38*
3.5.1.3 Sho1 Branch Module *38*
3.5.1.4 Integration on Pbs2 *39*
3.5.1.5 Hog1 Module *39*
3.5.1.6 Glycerol Module *39*
3.5.2 Information Transmission in the ΔSte11 Strain *40*
3.5.3 Information Transmission in the ΔSsk2/ΔSsk22 Strain *41*
3.6 Robustness and Sensitivity Analysis *41*
3.6.1 Robustness *42*
3.6.2 Sensitivity *44*
3.6.2.1 Sensitivity under Varying Stress Conditions *44*
3.6.2.2 Sensitivity of the System in Different Response Phases *48*
4 **Summary** *51*

Acknowledgments *56*
References *57*
Annex 1 *59*
Declaration of Independence *64*

1. Introduction

The yeast osmotic stress response and the HOG (High Osmolarity Glycerol) pathway generally associated with it are one of the most extensively studied systems in the yeast *Saccharomyces cerevisiae*.

Yeast cells, subject to extremely hostile environments under harsh conditions such as high osmolarity, show a tremendous capability to adjust themselves to these conditions. Evolution had optimized the HOG pathway to be able to react within minutes and to maintain a regular cell metabolism and growth under sustained pressure. Fascinated by the stupendous survivability of yeast cells, researchers have focused on *Saccharomyces cerevisiae*, common baker's yeast, as an animal model and began more than two decades ago to look into the biology of its osmotic stress response in order to unravel the mechanisms responsible for it.

In addition to identifying the key players in the pathway and elucidating their biochemical role through numerous experiments, a great deal of effort has been made by systems biologists to develop mathematical models of the pathway and to simulate conditions that cannot be reproduced in the laboratory, or can only be reproduced with difficulty. In this way, the systems biology community hopes to gain an even better understanding of the pathway, its crosstalk with other pathways in the yeast, its robustness against mutations and its evolution over millions of years. Such models may help researchers to design adequate experiments in order to verify their theoretical hypotheses. Since the yeast HOG pathway is related to other pathways in other organisms, the hope is that a clearer interpretation of the process will enable a better view of other systems and a better understanding of the underlying principals and mechanisms of biological systems as a whole.

This work involves creating precisely such a mathematical model. It relies to some extent on well accepted models of the HOG pathway, such as Klipp *et al* (2005) and Zhike *et al* (2009). The principal aims of this work were to examine the model under various degrees of osmotic stress and to explore the integration of the two branches of the osmotic stress response – the Sho1 branch and the Sln1 branch. Data on the response of the yeast to such conditions was obtained in experiments conducted by Macia *et al* (2009). In order to be deemed valid and reliable, the model is intended to

comply with the results of these experiments. Its validity is also confirmed by demonstrating that other features of the model, such as biophysical changes, are in line with other experimental data, and that the model is robust to perturbations of the initial concentration of its species. Information transmission in the system was investigated mathematically and a sensitivity analysis was performed in order to examine more closely the roles and importance of the species and parameters of the system. Additionally, this work hypothesizes the existence of a feed forward mechanism in the system and discusses a scenario in which such a mechanism might be important. As an example of an implementation of a feed forward mechanism candidate that could play a role in the system, Skn7 is introduced: a transcription factor already known to interact with the Sln1 branch that was previously only known to play a role in other pathways in the yeast and never shown to be involved in the osmotic stress response experimentally. This work is purely theoretical and as such it is meant to be used as a platform for further investigations and predictions of the behaviour of the yeast under various environmental conditions. Such predictions can be later confirmed in experiments and shed new light on the yeast's osmoadaptation and response to osmotic stress.

2. The Model

2.1 Model Graphical Presentation

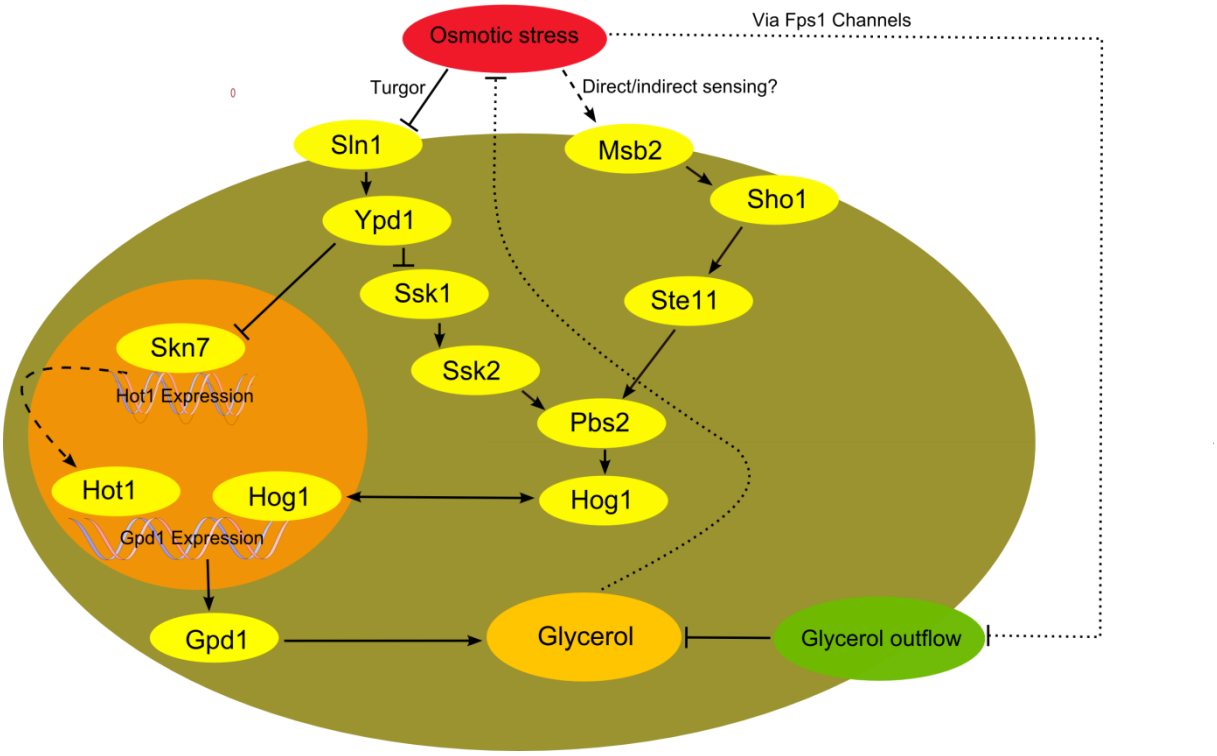

Figure 1: Model graphical presentation

Osmotic stress results in inactivation of Sln1 via turgor pressure, activation of Msb2 via direct or indirect sensing and closure of Fps1 due to changes in biophysical properties of the cell. Outflow of glycerol is reduced when Fps1 channels are closed. Both Sln1 inactivation and Msb2 activation lead to dual-phosphorylation of Pbs2 that in its turn phosphorylates Hog1. Dual-phosphorylated Hog1 enters the cell nucleus. Ypd1p enters the nucleus (not modelled here) and activates Skn7. Skn7 is hypothesized to regulate the expression of Hot1. Nuclear, dual-phosphorylated Hog1 and Hot1 act in concert in order to upregulate the expression of Gpd1. Gpd1 participates in the production of glycerol. Accumulation of glycerol due to glycerol production and reduced outflow give rise to increase of internal pressure and to relief of osmotic stress.

2.2 Biochemical and Mathematical Principles

Having understood the graphical representation of the model, a closer look is taken at the mathematical approach used to create this model, and the biochemistry on which it is based is discussed in detail.

For the quantification of the model, ordinary differential equations have been applied. The system of thirty differential equations, 55 parameters and six equations governing the biophysical changes the cell undergoes were assessed numerically using MATLAB. Matlab scripts can be found on the CD attached to this work.

The kinetics of the biochemical interactions in the model were chosen from a set of known kinetic models described in the literature (e.g. Mass-Action kinetic, Michaelis-Menthen kinetic and Hill kinetic) that justify, from a biological perspective, choosing them.

For biophysical changes, equations that are well accepted by the scientific community were chosen. As mentioned before, some of the equations were adopted from other models (e.g. Klipp *et al* [1]).

As to the parameter estimation, this was done by adopting parameters from other known models and estimating the unknown parameters while taking into consideration common principles and data from the literature [4, 5].

2.2.1 Model Inputs

The osmotic stress applied to the system is registered by proteins on the outer membrane of the cell. It was postulated that this could be sensed by at least two transmembrane proteins - Sln1 and Msb2 /Sho1/Opy2 [6, 7, 8]

Input for the Sln1 branch

Although the mechanism of sensing the osmotic stress is not yet fully understood, it is accepted that the Sln1 senses changes in turgor pressure [9]. Klipp *et al* assumed that there is a linear and proportional dependency between the salt concentration and the turgor pressure [see equations in Annex 1]. Sensing the turgor pressure by means of Sln1 was assumed to be linear, but proportional to an exponent thereof (in this model to the power of 4) as indicated in the equation below:

$$InputSln1\ (t) = \ k1 \cdot \left(\frac{turgor(t)}{turgor(t=0)}\right)^{k2}$$

Where k1 is a factor and k2 is the coefficient of the input

Input for the Sho1 branch

Whereas a lot is known about the input for the Sln1 branch, the input for the Sho1 branch remains elusive. It is not yet known which protein senses the branch, whether this involves one protein or more, which biophysical changes are sensed and whether these are intra- or extracellular. In this model, sensing by Msb2 was assumed. As in the case of Sln1, a turgor dependent input was modelled (see Annex 1). A few publications suggested activation independently of turgor pressure [7, 9] or suggested other means of activation, such as a direct sensing via changes in the environment's osmolarity or indirect sensing of changes in internal pressure, or volume change [7,10]. Although this work is based on the assumption that sensing of the turgor pressure occurs, the other possibilities are also discussed.

2.2.2 The Sln1 Branch

Via its input, the Sln1 branch transmits the changes in turgor pressure to Pbs2, which in turn transmits them to the MAP-kinase Hog1. It is considered to

be comprised of the phosphorelay system upstream in the branch, and Ssk2 (and its redundant protein Ssk22) and Pbs2 [4].

2.2.2.1 Phosphorelay

The phosphorelay module, its governing mass-action kinetics equations and their parameters were adopted from Klipp *et al* [1]. In general a phosphate group is passed back and forth between Sln1 and Yln1 and from Ypd1 to Ssk1 [11]. In cells under normal osmotic conditions, the members of the phosphorelay module are phosphorylated and become dephosphorylated upon osmotic stress. Hence, osmotic stress actually inactivates the branch. The system has been well studied and resembles the two-component system that can be found in many other organisms [12].

2.2.2.2 Ssk2-Pbs2-Pbs2p

The active, dephosphorylated, form of Ssk1 activates SSK2, and the redundant protein Ssk22. Upon activation Ssk2/Ssk22 undergo autophosphorylation [13]. For the activation of Ssk2 (for convenience and due to its redundancy Ssk22 was omitted from the model) a mass action kinetic was assumed. For the activation of Pbs2 and consequently Pbs2p (one-fold phosphorylated Pbs2) a Michaelis-Menthen-Kinetic (MMK) was assumed. In this model, the maximum concentration of Pbs2 is approximately 10 times greater than the maximum concentration of Ssk2. Although MMK requires a far greater concentration of substrate (in this case Pbs2) than of enzymes, an MMK in often used in biological systems regardless of this requirement [14].

2.2.2.3 Ypd1 as a Junction

Ypd1 interacts with both Ssk1 and Skn7. The latter is not considered to play a role in the Sln1 branch, but hypothesized to play an indirect role in the HOG pathway as will be explained later. The interaction of Ypd1 with Skn7 requires

Ypd1 to enter the nucleus. For reasons of clarity, this was not modelled. Janiak-Spens *et al* [5] characterized the interactions Ypd1-Ssk1 and Ypd1-Skn7, and measured the ratio between the forward and backward transfer of the phosphate group in these interactions. This ratio was taken into account in this model.

2.2.3 The Sho1 Branch

It is well established that HOG pathway can also be activated by the Sho1 branch [15, 16]. The Sho1 branch is known to play a role in other processes in the yeast [17], but the biological rationale for its involvement in osmoadaptation is not yet fully understood. However, there is some speculation regarding the distinctive roles of the two branches [4, 10]. Here a system comprising three proteins was modelled. These proteins recruit one another to form a protein scaffold upon activation. The spatial structure of the Sho1 branch is therefore quite different from the Sln1 branch, in which the proteins are freely located to the cytoplasm [15]. This may have implications on the integration of both branches at the level of Pbs2, as discussed in paragraph 3.4. As to the interaction of the three members of the branch, a mass action kinetic was assumed. The phosphorylation of Pbs2 was modelled, as in the case of the Sln1 branch, using MMK.

2.2.4 Skn7 and Hot1

As emphasized in 2.2.2.3, the role, if any, of the Skn7 protein in the osmotic stress response is not clear. It is known to play a role in other stress responses [18, 19]. There is, however, no doubt that it interacts with the phosphorelay system. One might assume that Skn7 influences the balance of phosphotransfer and therefore the whole HOG pathway at least passively, even without having an active role in the system. As the phosphotransfer is favoured 100-fold more towards Ssk1 [5], the passive role of Skn7 was not examined in the model. Instead, an active role was hypothesized as explained below:

Skn7 is a transcription factor of hundreds of genes [http://www.yeastract.com], including Hog1, Hot1 and many others. In light of these facts, it would be reasonable to believe that Skn7 does play a role, directly or indirectly, in the osmoadaptation.

A database search revealed that Skn7 regulates Hot1, a transcription factor considered to be involved in the regulation of genes that are responsible to glycerol production in response to osmotic stress [20]. Hot1 and Hog1 interact together with these genes [21].

Hot1 has only six known transcription factors from which 5 transcription factors play roles in totally different cell processes [http://www.yeastract.com]. Skn7 seems to be the only transcription factor for Hot1 that has any bearing on the HOG pathway due to its interactions in the phosphorelay system.

Given this circumstantial evidence, a hypothesis was constructed in which SKN7 is a transcription factor for Hot1, where the active form of Skn7 is the dephosphorylated form [22].

$$\frac{d}{dt}\,Hot1mRNA = k9 + k10 \cdot \frac{(Skn7/k11)^{k12}}{1 + (Skn7/k11)^{k12}} - k13 \cdot Hot1mRNA$$

Hot1 mRNA transcription. k9 is the basal transcription of Hot 1 gene, k10, k11 and k12 are the maximal rate, dissociation rate and Hill coefficient of the formation of Hot1 mRNA transcripts, respectively. K13 is the degradation rate of Hot1 mRNA.

Hot1 protein and the nuclear double phosphorylated Hog1 act in concert to regulate the transcription of Gpd1, an enzyme involved in the production of glycerol as will be discussed in paragraph 2.2.7

2.2.5 Pbs2

The signal from both branches converges to Pbs2, a MAPKK, well conserved from yeast to human [23]. It has two specific docking sites for Ssk2 (or the redundant Ssk22) and Ste11. Whereas Ssk2 is freely located to the nucleus,

the activation by Ste11 recruits Pbs2 to a scaffold containing Sho1 and later on Hog1. It is therefore clear that Pbs2 is not a sink for the two branches, but rather it has two activation profiles and different dephosphorylation rates. Phosphorylation by Ste11 was also modelled using MMK.

To the best of the author's knowledge, there is no experimental data available describing the dephosphorylation rates of Pbs2p and Pbs2pp. This model therefore assumes an equal rate of dephosphorylation for the wild type and the two mutants. Other possibilities are discussed further in paragraph 3.4

2.2.6 Hog1

Hog1 is central to osmoadaptation in the yeast [4, 25, 26]. It is a MAPK and conserved from fungi to human. The time courses for Hog1 form the common estimator for the behaviour of the system both in experimental and theoretical research. Dual-phosphorylated Hog1 either enters the nucleus and participates as a transcription factor in the expression of glycerol producing genes, or, in its cytosolic form, participates in the metabolism of glycerol (not simulated in this model). The model structure of Klipp *et al* was adopted. It entails five states of Hog1 and a cytosol-nucleus shuttle system. For the phosphorylation of Hog1, Michaelis Menthen Kinetic was assumed.

2.2.7 Glycerol Production and Outflow

Glycerol is the molecule that the yeast cell uses to counteract the osmotic imbalance between the intra- and extracellular milieu resulting in the outflow of water and shrinkage of the cell [4].

An incline in glycerol concentration is achieved in two ways:

- Closure of the Fps1 channels to prevent outflow of glycerol.

There has been much speculation as to which elements signal the channels to close. A possible involvement of Hog1 in this process was also suggested, but could not be shown [26, 27]. Rather, a dependency on biophysical properties seems to deliver the simplest explanation. Due to the multi-unit structure of channel proteins [26] it was decided to model them using a cooperative, switch-like Hill kinetic.

- <u>Upregulation of the expression of genes that promote the synthesis of glycerol.</u>

  Production of glycerol is dependent on genes that are regulated by Hog1 [30]. The regulation also involves Hot1 as a recruiting factor for the RNA polymerase II [21, 28]. One protein, Gpd1, was chosen to represent these glycerol-producing genes. Its transcription is modelled similarly to the transcription of Hot1, but in an equation that involves two effectors – Hog1 and Hot1 [30].

$$\frac{d}{dt}\,Gpd1mRNA = k44 + k45 \cdot \frac{(Hog1ppNuc \times Hot1/k46)^{k47}}{1 + (Hog1ppNuc \times Hot1/k46)^{k47}} - k48 \cdot Gpd1mRNA$$

Gpd1 mRNA transcription. k44 is the basal transcription of Gpd1 gene, k45, k46 and k47 are the maximal rate, dissociation rate and Hill coefficient of the formation of Gpd1 mRNA transcripts, respectively. k48 is the degradation rate of Gpd1 mRNA

Both methods of increasing the concentration of Hog1 in the model were incorporated into one equation:

$$\frac{d}{dt}Glycerol = k51 \cdot Gpd1 - k52 + k53 \cdot \frac{((1 - turgor(t))/k54)^{k55}}{1 + ((1 - turgor(t))/k54)^{k55}}$$

Glycerol concentration in the cell

Glycerol production is the left term of the equation. A constant outflow rate for glycerol is represented by k52. The right term of the equation represents the retention of glycerol in the cell due to closure of the Fps1 channels and upon

induction of osmotic stress. k53 must be equal to or smaller than k52, since the channel must not contribute to production of glycerol.

As mentioned before, Hog1 is known to play a role in the regulation of the glycerol metabolism. This however was not modelled here.

2.2.8 Biophysical Changes

The governing equations for the biophysical changes in the model were adopted from Klipp *et al* and are attached in Annex 1.

2.2.9 Initial Conditions and Parameters

The initial conditions were taken from the literature [http://www.yeastgenome.org/].

Many parameters were adopted from Klipp *et al* and Zhike *et al*. Others, such as the phosphorylation rates of Skn7, were taken from publications [5]. Reasonable parameters for the mRNA transcription were chosen in accordance with the literature [31]. The parameters for the Sho1 branch and other equations were determined by simulating the model.

2.2.10 Sensitivity Analysis

In order to examine the influence of certain parameters on the model and to compare the behaviour of the wild type and the two branches, a sensitivity analysis was performed.

The sensitivity of a variable x (e.g. Hog1 concentration in the nucleus) dependent on a parameter p (e.g. Hog1 transfer into the nucleus) is defined as:

$$sensitivity\{x,p\}(t) = \frac{dx(t)}{dp} \times \frac{p}{x(t)}$$

The left term $\frac{dx(t)}{dp}$ represents the change in e.g. Hog1 concentration at a given time point *t* when the parameter p is perturbed.

The right term $\frac{p}{x(t)}$ is a normalization factor that makes the sensitivity independent of the size of x and p and makes it possible to express the sensitivity in arbitrary units.

In order to calculate the sensitivity, PottersWheel, a MATLAB® toolbox for mechanistic mathematical modelling, was used [http://www.potterswheel.de/].

The equation was numerically approximated with:

$$sensitivity\{x,p\} = \frac{(x(a \times p) - x(p))}{(a-1) \times p} \times \frac{p}{x(t)}$$

Where the factor a = 1.001

2.2.11 Normalization

The time courses of the species in the simulation do not take into account the changes in the volume of the cell during the experiments. In order to reflect the species' true concentrations, one must normalize these concentrations with the current cell volume at each point in time:

$$x(t)_{normalized} = x(t) \times \big(23.2 + Volume(t)\big)/(23.2 + Volume(t=0))$$

Where 23.2 fL is the fixed part of cell volume that is not affected by osmotic changes.

3. Results

3.1 Modelling Experimental Data

The main scope of this work was to gain insights into the yeast's response to various levels of osmotic stress and into the integration of both the Sho1 and Sln1 branches. In order to achieve this, the first step was to find suitable experimental data and then model it adequately. Macias *et al* [3] conducted experiments that tested the response of the pathway under varying salt concentrations of 0.07, 0.1, 0.2, 0.4, 0.6 and 0.8 Mol NaCl in the wild type and cells lacking either the Sln1 or the Sho1 branch (ΔSte50 strain and ΔSsk2/ ΔSsk22 strain, respectively). Since this model does not include the Ste50, it was decided to shut down Ste11 instead. Shutting down either branch was achieved by multiplying the equations involving Ssk2 or Ste11 by zero.

3.1.1 ΔSsk2/ ΔSsk22 Strain

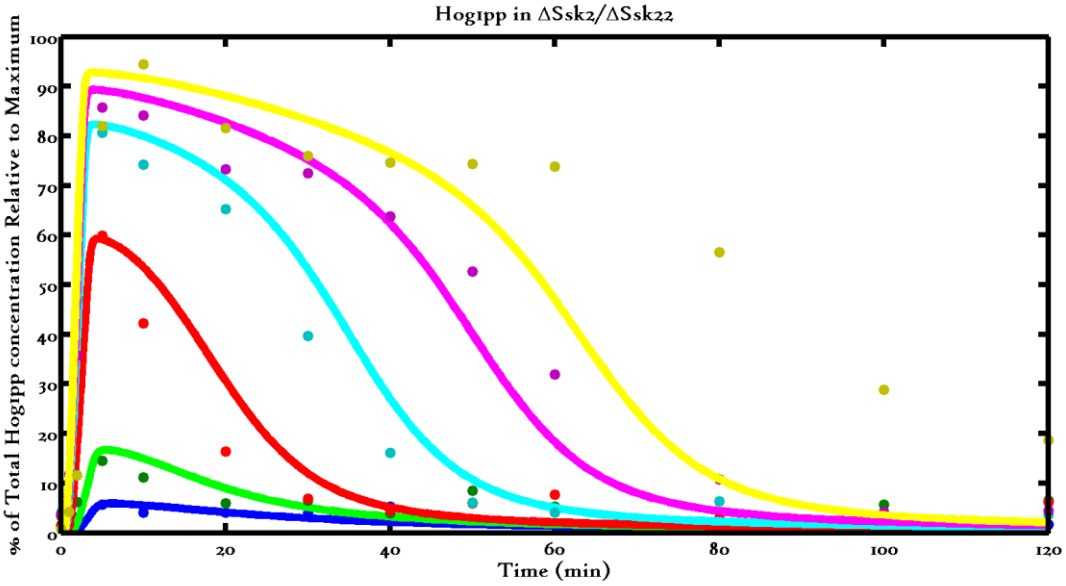

Figure 2: Yeast mutant lacking SLN branch activity (ΔSsk2/ ΔSsk22 strain). Time courses for dual-phosphorylated Hog1 (Hog1pp cytosolic + Hog1pp nuclear) under various degrees of osmotic stress (0.07, 0.1, 0.2, 0.4, 0.6 and 0.8 Mol NaCl) are plotted (blue, green, red, cyan, magenta and yellow, respectively) as the percentage relative to the maximum Hog1pp concentration in the wild type.
The dots represent the experimental data obtained by Macia *et al* [3] and the lines represent the simulation.

Apart from the response to the strongest stress (0.8 Mol salt), the model seems to describe the experimental results adequately. A rather gradual incline (especially with regard to the response to weaker stresses) and non-

saturation of the phosphorylated Hog1 can be observed. For yeast cells lacking the Sln1 branch, the switch-like accumulation of Hog1pp is devoid in response to weaker stresses.

There are however certain shortcomings to the simulation:

- For all salt concentrations, the concentrations of Hog1pp after 120 minutes are higher than those observed in the experiment. Nevertheless, in the model one can still observe that the higher the NaCl concentration applied, the higher the concentration of Hog1pp after 120 minutes.
- This is particularly true in the case of the response to 0.8 Mol NaCl. The concentration of Hog1pp after 120 minutes obtained experimentally is approximately 18% of the maximal concentration whereas in the model it is approximately 8%.

Alternative possibilities for input sensing in the Sho1 branch

In modelling the inputs for both branches, a dependency on the turgor pressure was assumed. Whereas such a dependency was shown experimentally for the Sln1 branch [7], the nature of osmo-sensing in the Sho1 branch is not clear [9]. Tatebayashi *et al* [7] suggested dependency on other biophysical changes in the system. They conducted experiments that suggested that the sensor for the branch activation can be either the cytoplasmic domain of Msb2, or non-cytoplasmic domains (TM and extracellular domain), where the latter requires the TM domain of Sho1.

A direct sensing of changes in the environment via the extracellular domain of Msb2 is an interesting possibility but raises a problem with regard to negative feedback and adaptation of the system. As the osmolarity of the environment does not change when the cell produces glycerol to counteract the intra- and extracellular pressure difference, the extracellular domain of Msb2 alone would not be able to sense the intracellular changes. The adaptation of the cell, in this case, could only be achieved via an intracellular negative feedback downstream of the stress-sensing molecule, Msb2.

Sensing via the cytoplasmic domain of the Msb2 protein could be achieved by measuring the changes in cell volume, or changes in the intracellular pressure. What structural changes an Msb2 would undergo is an interesting question, but beyond the scope of this work.

In order to check if the input can be modelled dependent on the cell volume or internal pressure, the input equation [equation…] was replaced with equations that describe dependency on cell volume without changing or tuning any other parameter or equation in the model.

$$input(t) = \frac{Volume_{(t=0)}}{Volume(t)^{2.5}}$$

Or internal pressure:

$$input(t) = \frac{Internal\ Pressure\ (t)}{100}$$

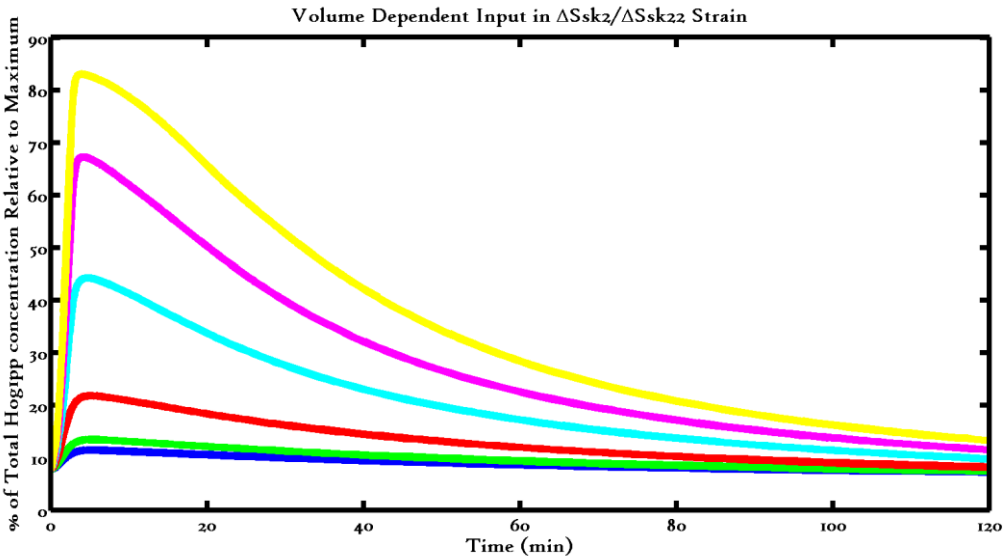

Figure 3: Volume dependent input in theΔSsk2/ ΔSsk22 strain.

The main attributes of the response, namely the graded incline and decline and the almost perfect adaptation are preserved (compare with figure 2). Tuning the model parameters without changing them profoundly would be sufficient to achieve an adequate description of the experimental data.

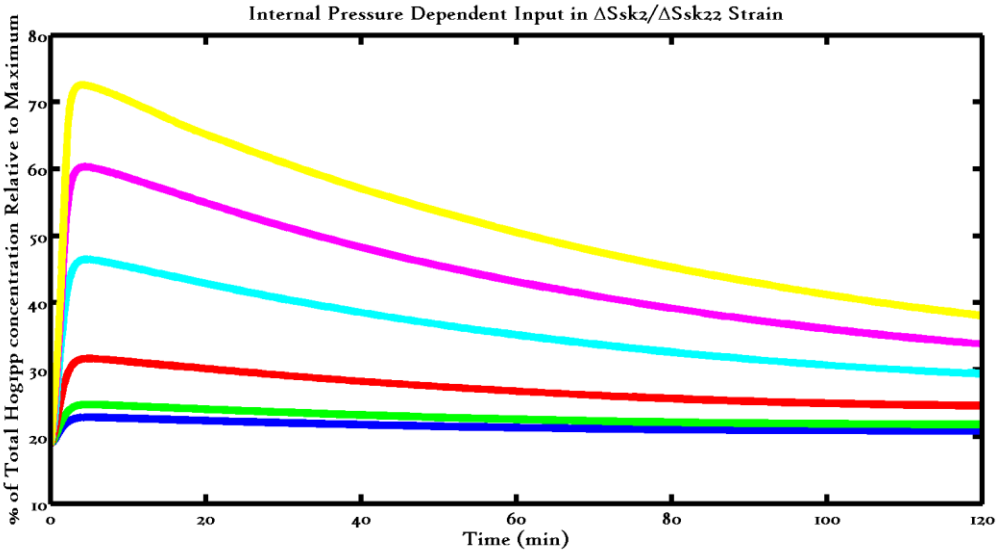

Figure 4: Internal pressure dependent input in theΔSsk2/ ΔSsk22 strain.

Modelling the input dependent on the internal pressure results in a graded response but the adaptation is not as effective as when dependent on turgor or volume change. An adequate description of the experimental data would require more changes to the model.

3.1.2 ΔSte11 Strain

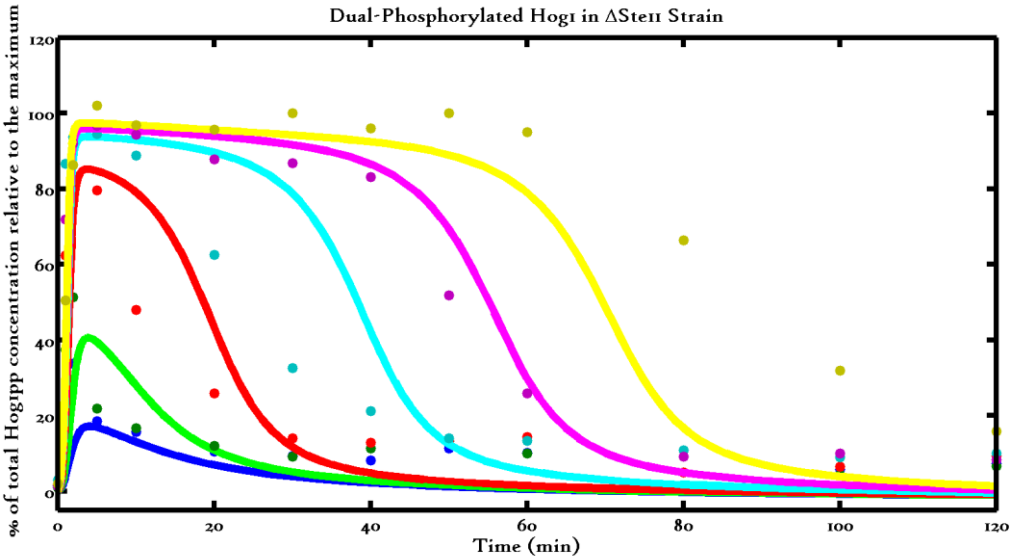

Figure 5: Yeast cells lacking Sho1 branch activity. For this purpose the ste50 protein was knocked out. Data and simulation representation are as for Figures 2-4.

The ΔSte11 strain shows a different response to osmotic stress than the ΔSsk2/ ΔSsk22 strain. Hog1pp reaches almost 100% of the concentration in the wild type. There are a few shortcomings to the model when compared to the experimental data:

- Although the Hog1pp accumulation under the lowest stresses (0.07 and 0.1 Mol NaCl) are quite similar in the model and experimental data (reaching up to 30% and 50% of the maximum, respectively), the incline of the Hog1pp concentration under the two lowest stresses is much more rapid in the experiments than in the model. The same goes for the decline
- As in the ΔSsk2/ ΔSsk22 strain, the cell adapts to 0.8 Mol NaCl too quickly.
- For the ΔSte11 strain, the cell adapts too slowly to (0.4 Mol NaCl).

3.1.3 Wild Type Simulation

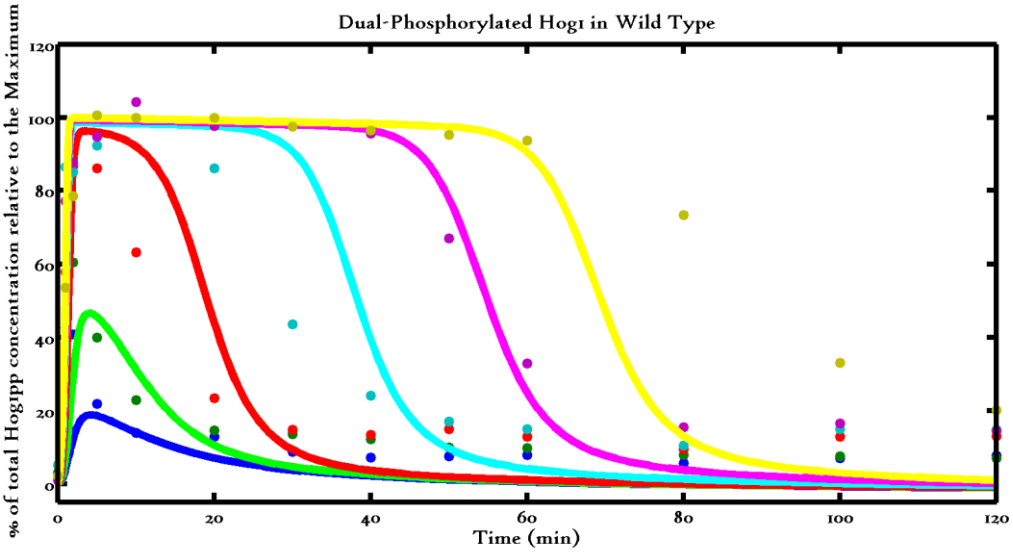

Figure 6: Dual-phosphorylated Hog1 proteins in the wild type. Data and simulation representation are as for Figures 2-5.

In the wild type, a saturation of the Hog1pp concentration is clearly observable for the response to the three highest concentrations – 0.4, 0.6 and 0.8 Mol NaCl. As

to the switch-like incline Hog1pp concentration, it is more similar to the incline in the ΔSte11 strain than to the ΔSsk2/ ΔSsk22 strain

Shortcomings:

- The response of the system to the two lowest salt concentrations is still not as rapid and as strong as the response seen in the experimental data.
- As with the other two strains, the system adapts to the highest stress too quickly.
- As with the ΔSte11 strain, adaptation to 0.4 Mol NaCl begins too lat

3.2 Species' Properties and Kinetics

As shown in 3.1, the model describes the experimental data obtained by Macia et al. in an adequate manner. However, in order to be deemed valid, the model must accord with further experimental data and generally accepted biological principles.

In this chapter, experimental data from two publications – Klipp *et al* [1] and Muzzey *et al* [32] – will be presented and the model's compliance with them will be discussed.

3.2.1 Biophysical Changes

Biophysical properties such as glycerol accumulation and changes in cell volume are documented in the literature. The model's compliance with the experimental results is shown below.

3.2.1.1 Glycerol Intracellular Concentration

The accumulation of the intracellular concentration of glycerol as a response to an osmotic shock of 0.5 Mol NaCl was measured by Klipp *et al* [1]:

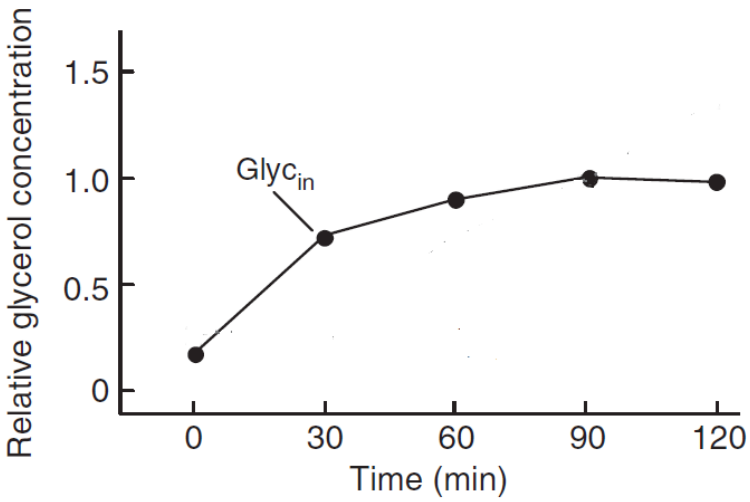

Figure 7: From Klipp *et al.* Glycerol intracellular accumulation as a response to osmotic stress

The model predicts the intercellular concentration adequately:

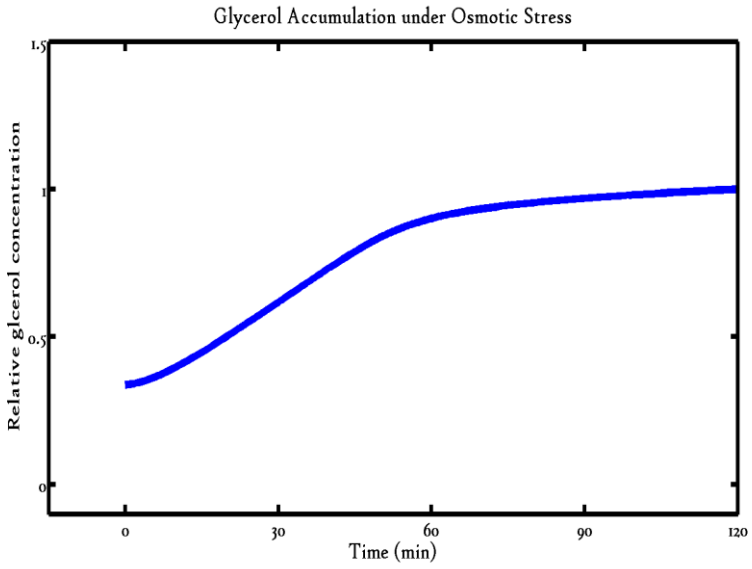

Figure 8: Accumulation of intracellular glycerol in the model

3.2.1.2 Cell Volume

Muzzey *et al* [32] measured the changes in cell volume under osmotic stress of 0, 0.2, 0.4 and 0.6 Mol NaCl (black, blue, green and magenta lines, respectively):

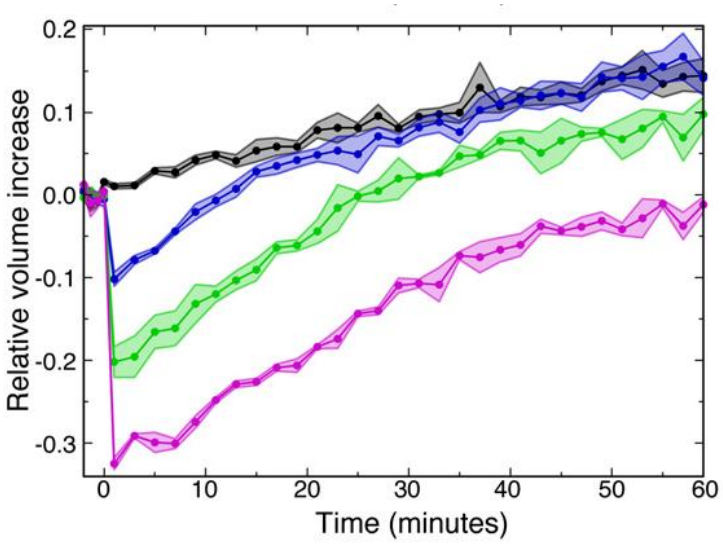

Figure 9: From Muzzey *et al*. Relative volume increase in the cell under 0, 0.2, 0.4 and 0.6 Mol NaCl (black, blue, green and magenta lines, respectively)

The experimental data shown here raises a question with regard to the behaviour of the cell in the absence of osmotic stress. Muzzley measured an increase up to 10% of the original cell volume during 60 minutes under 0 Mol NaCl (black line). In the model, a steady state for all species was assumed under 0 Mol NaCl.

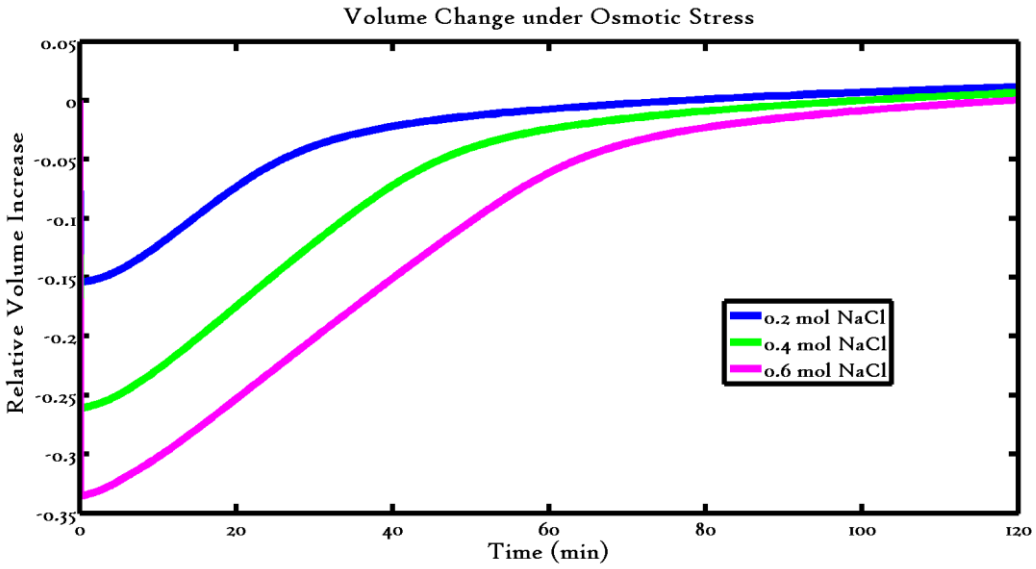

Figure 10: Relative volume increase in the model.

The model predicts the changes in volume well, in terms of relative values. However, an overshoot is not observed in the model.

3.2.2 Fps1 Mutant

Fps1 is a channel protein that is involved in the uptake of chemicals such as arsenite or antimonite [33] and in the response to stress induced by acetic acid [33]. In the osmoadaptation it was shown to control the efflux of glycerol [26, 27]. In Klipp *et al*, mutant yeast cell that are not able to close the Fps1 channels were examined:

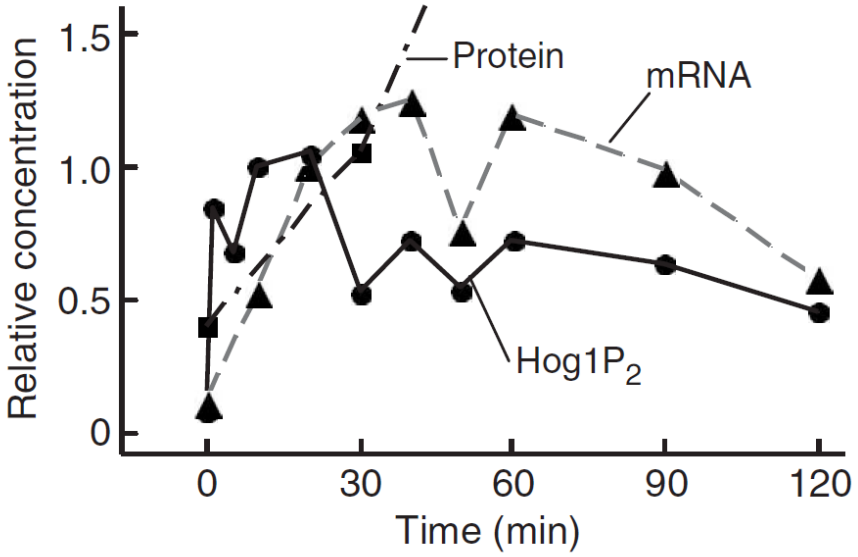

Figure 11: From Klipp *et al*: Response of yeast cells that are not able to close their Fps1 channels to 0.5 Mol NaCl. The time course for the mRNA shown in the figure refers to SLT1 mRNA which was not modelled in this model. The protein is Gpd1.

The Fps1 protein was not explicitly modelled in this work's model. However, the equation for the glycerol concentration contains a term which describes the channel activity.

Eliminating this term will model a shut-down of the channels' closing apparatus:

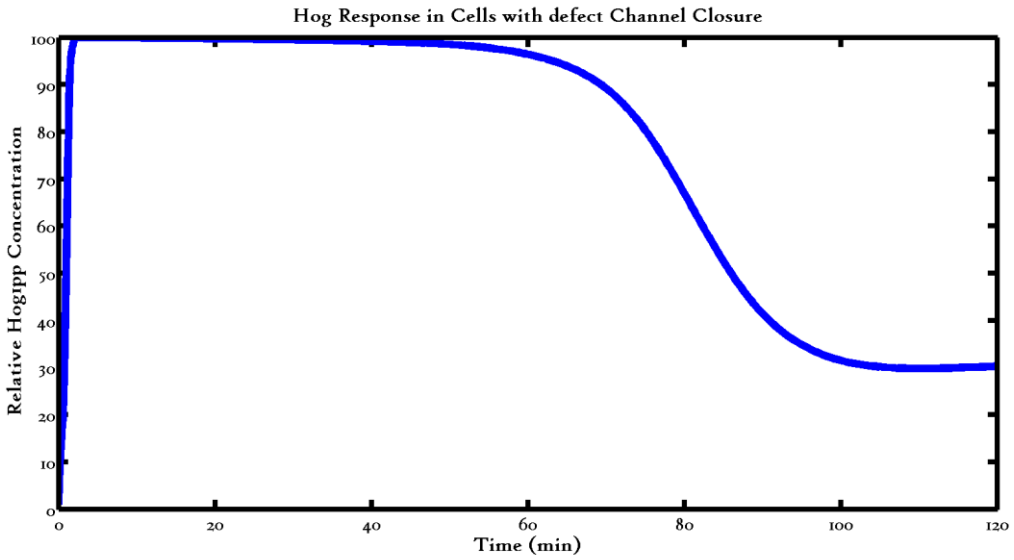

Fig 12: Relative concentrations of total Hog1pp in the model lacking channel activity

The inability of these channels to adapt adequately is clearly observable here. Hog1pp concentration reaches 30% of maximum concentration after 120 minutes.

3.2.3 mRNA Species

Rep *et al* [28] have measured the concentration of mRNA and protein species after induction of osmotic stress.

Under 0.7 Mol NaCl, the concentrations were estimated to be about threefold higher than in cells that grow under normal conditions. It was also observed that the concentration of mRNA is highest 45 minutes after the induction of osmotic stress. These properties are well described by the model.

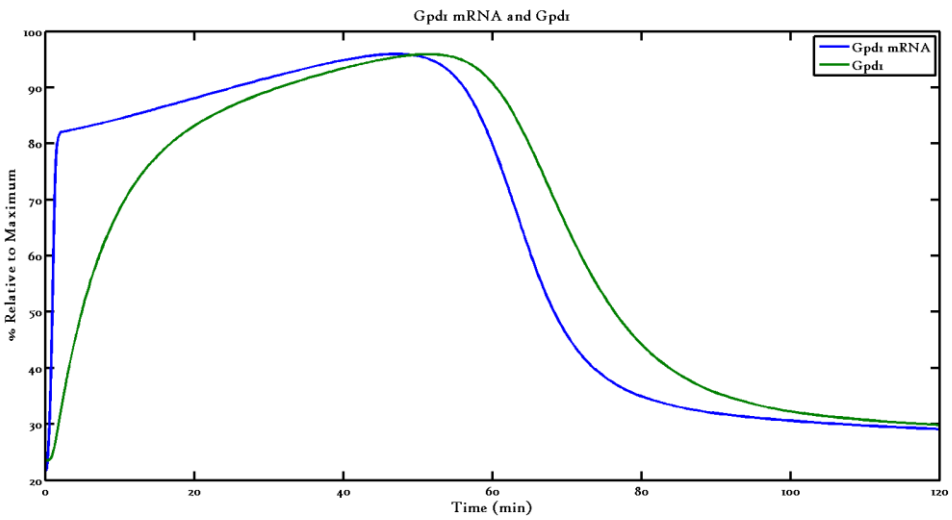

Figure 13: Concentration of Gpd1 mRNA and protein in presence of 0.7 Mol NaCl

Concentrations of both species are fourfold higher in response to osmotic stress of 0.7 Mol NaCl. There is, however, a shortcoming in the model – the mRNA concentration inclines too quickly. One would expect a more gradual incline, since the expression of a Hog-dependent mRNA should occur 20 minutes after Hog1pp accumulates.

3.3 The Feed-Forward Mechanism

Complicated biological systems contain internal regulation loops that allow the systems to finely regulate their response to conditions imposed by the environment surrounding them [35, 36].

3.3.1 Hot1 mRNA Regulation as an Example of a Hypothetic Feed-Forward Mechanism

In this work, a feed-forward mechanism is suggested. Whether, how and to what extent such a mechanism would contribute to the osmoadaptation of the yeast is introduced and examined in this section.

Mettetal *et al* [37] examined the impact of subsequently applied stresses on the system in the following design:

- Four groups of yeast cells were subjected to osmotic stress in different levels (0.1, 0.2, 0.35 and 0.5 Mol NaCl) for a period of time (8, 16, 22.5 and 30 minutes respectively).
- After each period of time, the cells were washed and placed in a NaCl-free medium for the same amount of time (8, 16, 22.5 and 30 minutes respectively).
- The experiment was repeated four times for each stress level.

The results show a trend in which the system adapts to osmotic shock better the higher the NaCl concentration:

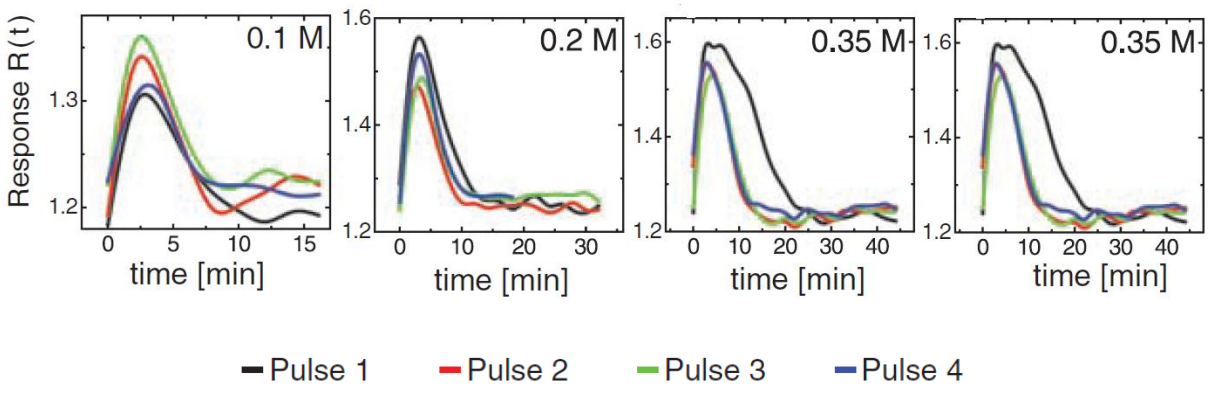

Figure 14: from Mettetal et al. 2008. The Hog1pp response of four cells groups was measured for four stresses in four alternating periods of time: stress-non stress.

The issue here is to identify what is responsible for this phenomenon. Mettetal raised the possibility that the effect might be connected to genes regulated by the nuclear Hog1pp. To investigate the effect of such genes, he conducted the same experiment but with cells that were treated with cycloheximide – a compound that blocks the translation of mRNA to proteins.

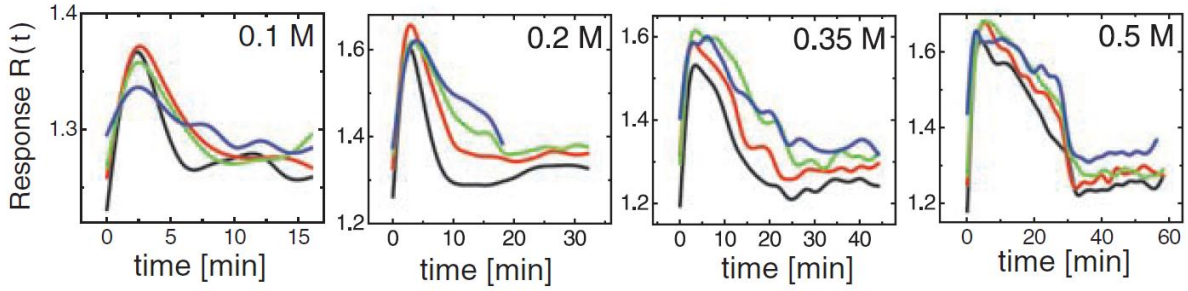

Figure 15: From Mettetal 2008. The results of the same experiment, this time with cells that were first treated with cycloheximide.

Whereas the adaptation to 0.1 Mol NaCl is similar in all four stress-non stress pulses, the adaptation to higher stresses becomes less effective the higher the stress.

In view of these results, Mettetal concluded that gene expression plays a role in long time scales and intense shocks.

mRNA decay rates are considered to be less dependent on their degrading proteins, the nucleases, and more dependent on their intrinsic properties and the function of their peptide products [38]. It is therefore logical to assume that an increase in the concentration of mRNA will result in a proportional rise in the product.

An increase in the concentration of Gpd1 mRNA will result in an overproduction of glycerol as shown in the literature [39]

Overproduction of glycerol is uneconomical for the yeast cell and needs to be avoided. Hence, it is beneficial for the yeast to regulate the expression of Gpd1 mRNA in a way that is closely tied to the Hog1 adaptation.

In view of these considerations, it would be rather implausible to make the expression of the glycerol regulating proteins accountable for the phenomena observed by Mettetal.

Rep *et al* [20] studied the effect of a Hot1 mutant on the expression of a few hundreds of genes. The genes that were found to be down-regulated by Hot1, among them the Gpd1 gene, are also known to be regulated by Hog1. Therefore it was concluded that Hot1 interacts together with Hog1 in concert, in order to regulate the expression of Gpd1 and other genes. This premise was later confirmed in other publications [21] [40].

Since accumulation of Hog1 is necessary for the regulation of Hot1-regulated genes, accumulation of Hot1 mRNA and Hot1 protein per se would not lead to

unwanted up-regulation of Gpd1, glycerol accumulation and a waste of resources.

These considerations make it plausible to assume the involvement of Hot1 in better adaptation of the Hog1 signal under intense osmotic condition and over a long period of time.

Whereas all the species in the model adapt in synchronization with Hog1pp, Hot1 mRNA concentration stay high after the system has adapted:

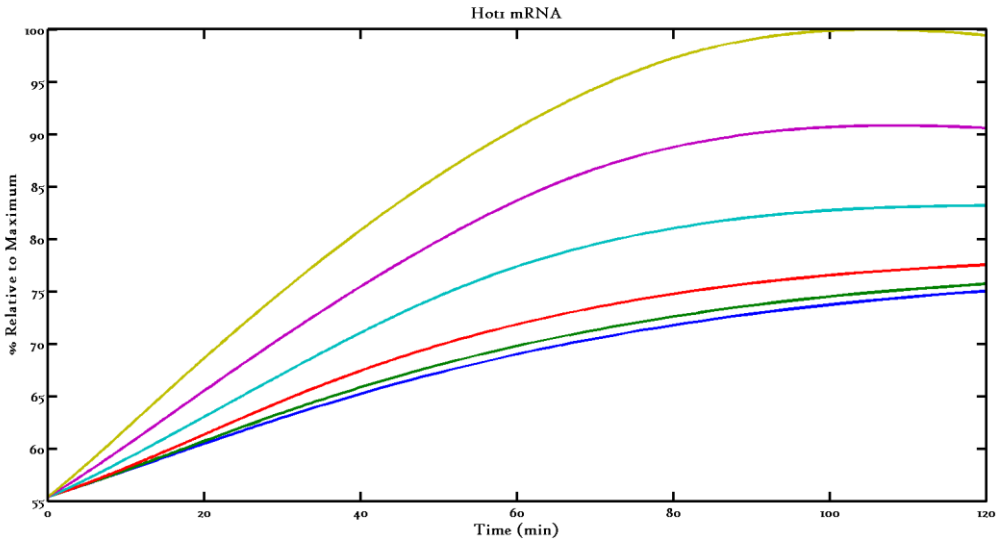

Figure 16. Time courses for Hot1 mRNA under various degrees of osmotic stress (same degrees as in Figures 2-6)

One observes that Hot1 concentration reaches its peak long after Hog1 starts to decline.

In order to test the effect of the rise in the concentration of Hot1 mRNA on the adaptation and to compare it to Mettetal's results, a simulation was run with the same four stress levels (0.1, 0.2, 0.35 and 0.5 Mol NaCl). Since Mettetal washed the cells after each stress pulse and left the cells in an environment with normal osmolarity, it was assumed that all initial species concentrations were reset to their initial value after each stress pulse, apart from the value for Hot1 mRNA. The same was done in the simulation – after each stress pulse the initial species concentrations were set back to their original values, apart from the Hot1 mRNA concentration, which was increased by a factor of 1.5.

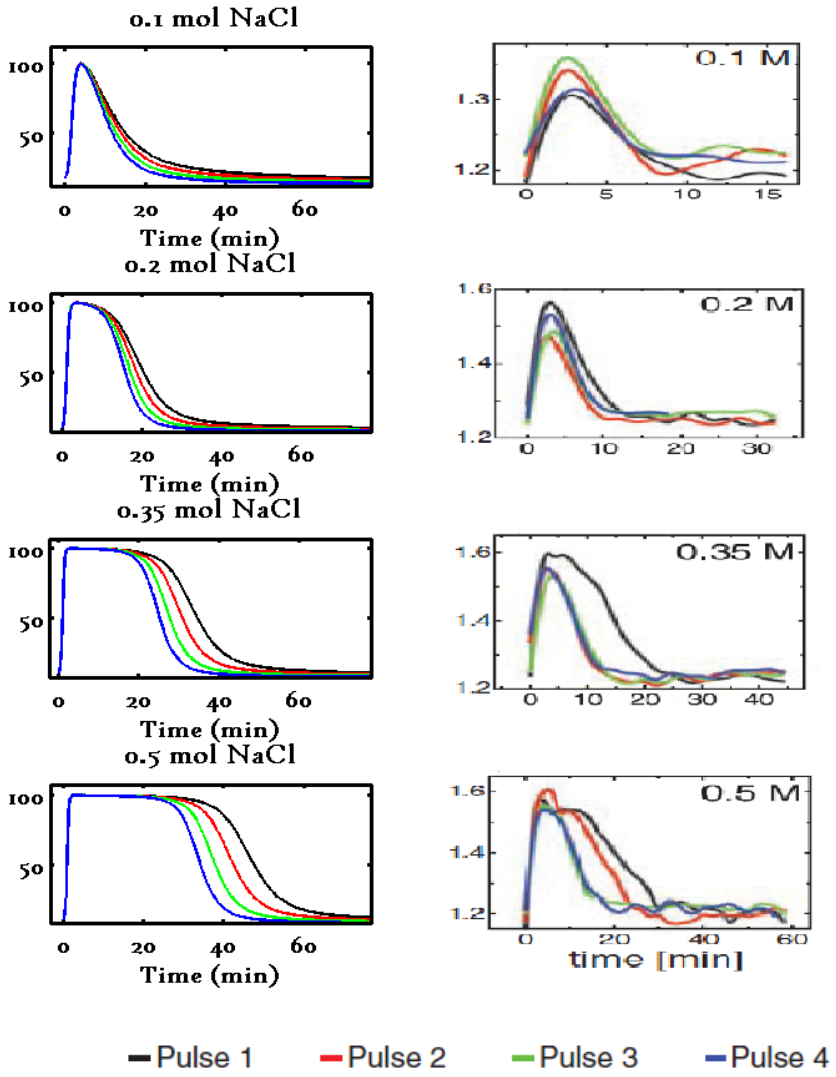

Figure 17: dual-phosphorylated Hog1 accumulation resulting from consecutive stress pulses. Right – from Mettetal et al 2008. Left – model simulation.

From the figure, one can easily conclude that the stronger the stress, the better the system adapts to subsequent pulses of the current stress.

Designing a simulation that describes the other experiment in the publication, in which the whole mRNA expression was eliminated using cycloheximide, was not possible. In the model, the production of glycerol is dependent on the mRNA and protein formation of Hot1 and Gpd1. Eliminating it would result in a complete inability to adapt to osmotic stress.

3.3.2. Effects of Skn7 on the Osmoadaptation

Skn7, its involvement with the phosphorelay system and the regulation of Hot1 mRNA was introduced in the introduction. Hot1 mRNA expression was

suggested as a feed forward mechanism in the previous section. Skn7 was modelled here to regulate the expression of Hot1 based on circumstantial evidence from the literature. Although not yet investigated under osmotic stress, a ΔSkn7 strain is known to be at least viable [41]. Therefore eliminating Skn7 was modelled here to have only a minor impact on the cell's behaviour under osmotic stress.

It is important to mention that the data generated by Macia *et al* [3], on which this work relies, does not affect Skn7 whatsoever. In order to shut down the Sln1 branch, Macia used a ΔSsk2/ΔSsk22 strain. These two redundant proteins are located further downstream from the phosphorelay module to which Skn7 belongs. Hence, a comparison is possible between Macia's data and the simulations for the wild type and the Skn7 mutant, as shown in the figure below:

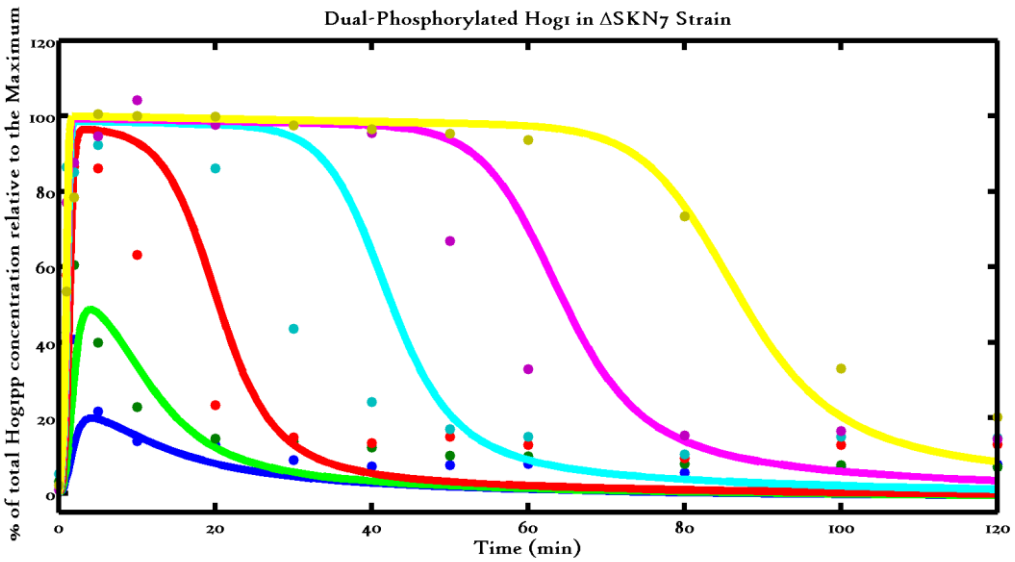

Figure 18 : Accumulation of dual-phosphorylated Hog1in ΔSkn7 strain

There is only a minor difference between the simulations of both strains. The wild type clearly adapts slightly faster than the ΔSkn7 strain (compared to Figure 6). On the other hand, one can observe that in the ΔSkn7 strain, Hog1pp adapts less effectively than the wild type and in a way that is more similar to the experimental results.

3.4 Integration of Sln1 and Sho1 Branches

The Sln1 and Sho1 branches converge at the level of the MAPKK Pbs2. These branches are, as shown in the model scheme, spatially distinct and controlled by different sensors [4]. Moreover, the proteins in one branch do not appear to crosstalk with the proteins of the other branch [15].

An interesting question that has not been investigated so far (at least not in a mathematical model approach) is how the integration on the Pbs2 level occurs.

The Pbs2 protein has three binding partners (Ssk2, the redundant ssk22 and Ste11, all in a phosphorylated form) and is considered to act differently with regard to the two branches [13] [24].

Its interaction with the active Ssk2/Ssk22 (Ssk2p/Ssk22p) is characterized as a MAPKKK-MAPKK interaction – the signal is passed from the active form of Ssk2/Ssk22 to Pbs2 by means of phosphorylation. Ssk2/Ssk22 can then either become inactivated or phosphorylate the next Pbs2 molecule [42].

Phosphorylated MAPKKK Ste11 (Ste11p) phosphorylates Pbs2, thereby recruiting it to a protein scaffold to which Hog1 and Sho1 are also recruited [15, 43].

The behaviour of both branches is different, yet according to the experimental data for the mutants, obtained by Macia, both are being activated even when low stresses are applied (although to different degrees).

Therefore it would be reasonable to assume that both are active in the wild type (unless some unknown inhibitory crosstalk between members of one branch prevents phosphorylation of Pbs2 by a member the other branch).

In the figure below, the experimental data obtained by Macia is presented slightly differently in order to emphasize the similarity and dissimilarity between the three strains (WT, ΔSsk2, ΔSte50).

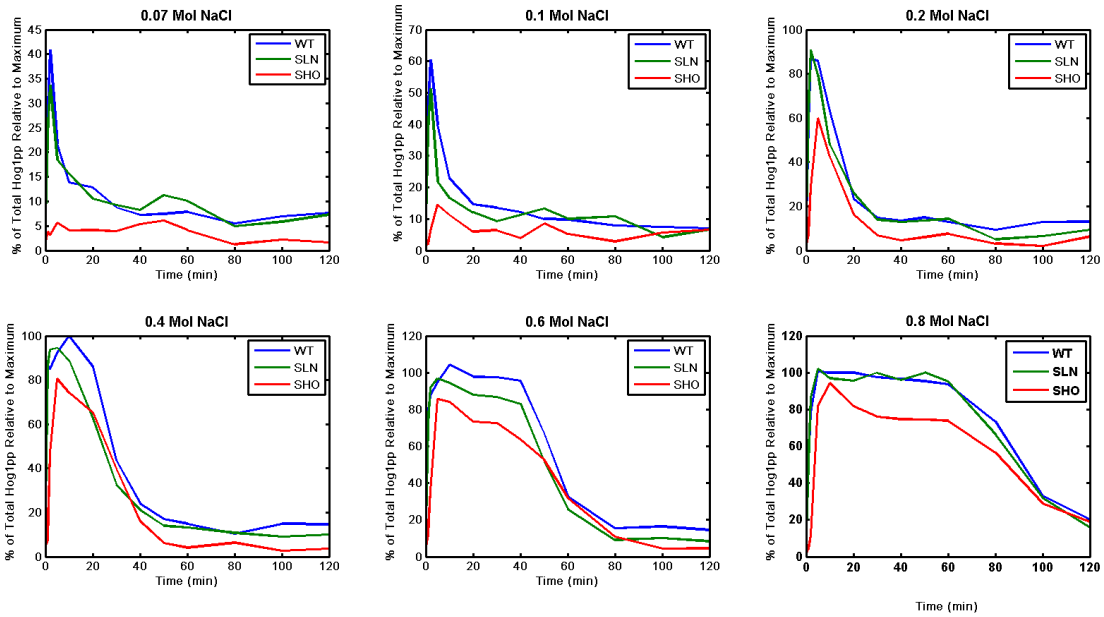

Figure 19: Macia's data in a different presentation – for each stress all three strains – WT, ΔSsk2, ΔSte50 are plotted

The time course for the wild type is, for most of the stresses, almost identical to that of the ΔSte50 strain. The Sho1 branch does not appear to contribute (or only to a minor extent) to the response of the system.

In the model, one can observe the same trend, but the time courses of the SIn1 and the wild type are not as similar as in the experimental data, especially with regard to higher levels of stress:

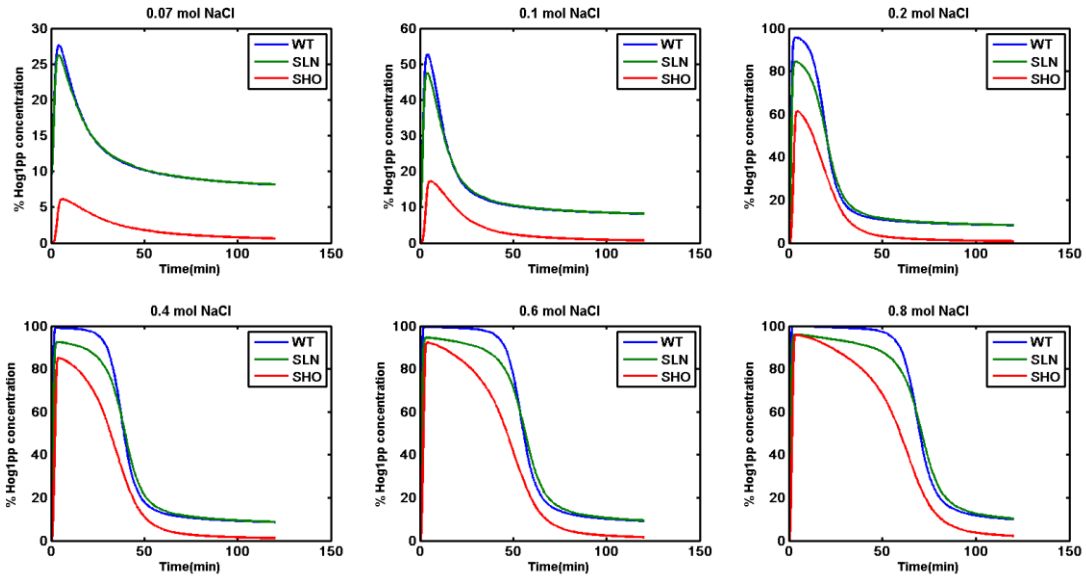

Figure 20: Simulated Hog1pp response with similar presentation as in Figure 19.

Due to the distinction between the two branches and the fact that no crosstalk upstream from Pbs2 is known, it was decided to integrate the branches in an additive manner – the equations for the phosphorylation and dephosphorylation of Pbs2 were simply added to each other.

The equations for phosphorylation of Pbs2 by Ssk2/Ssk22 or Ste11 have different parameters, as expected in view the different nature of phosphorylation (see introduction)

The dephosphorylation rates for Pbs2pp are unknown – both forms of Pbs2 might share the same phosphatase or use different ones. Therefore it was decided to use the same general degradation rate for all three strains. In this section the possibility that the degradation rates are not the same for both branches and the wild type will be discussed.

For the Sho1 branch at least, in which Pbs2 is recruited to the protein scaffold, there is some additional information with regard to the dephosphorylation of Pbs2. It involves the Nbp2 protein, which negatively regulates the HOG pathway by recruiting the phosphatase Ptc1 to the Sho1-Pbs2-Hog1 scaffold. The Ptc1 inactivates the scaffold [44]. Deletion of Nbp2 disrupts the Pbs2-Ptc1 complex, thereby increasing Hog1pp concentration and impairing adaptation [45]. The total number of Nbp2 molecules is fourfold lower than the total number of Pbs2 molecules [http://www.yeastgenome.org/]. Moreover, the Nbp2 molecules are located to both nucleus and cytoplasm whereas Pbs2 is only located to the cytoplasm.

Therefore in the ΔSsk2/ ΔSsk22 strain, in which all Pbs2pp molecules are recruited to the scaffold, the Nbp2 protein might act as a limiting step in the inactivation of the scaffold. In a wild type, in which both branches are active, the overall inactivation of Pbs2 would be less affected by the limiting step in the Sho1 branch (assuming there is no limiting step in the Sln1 branch) and therefore higher than the sum of the dephosphorylation rates for each branch alone.

The following figure shows the behaviour of the system when the dephosphorylation rate of Pbs2 in the wild type is higher than the sum of the dephosphorylation rates of both branches:

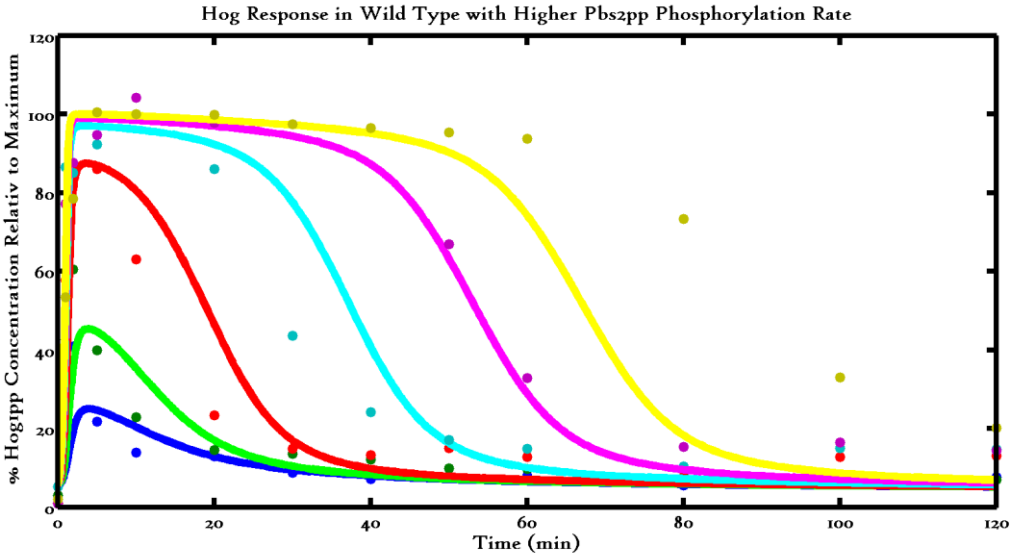

Figure 21: Time courses for dual-phosphorylated Hog1 in wild type. Dephosphorylation rate for dual-phosphorylated Pbs2 was raised.

Compared to Figure 6, a higher dephosphorylation rate for the wild type describes the experimental data for an osmotic shock of 0.2 and 0.4 Mol NaCl in a more adequate manner. The simulation in the figure below presents the results of the simulation with emphasis on the degree of similarity in the response of the three strains to different levels of osmotic stress (as in Figures 19, 20), compared to the situation of equal dephosphorylation rates for the three strains (see Figure 20). One can observe a greater similarity of the figure below to the experimental data of Macia (see Figure 19), at least for the phase of the response in which the Hog1pp concentration is high.

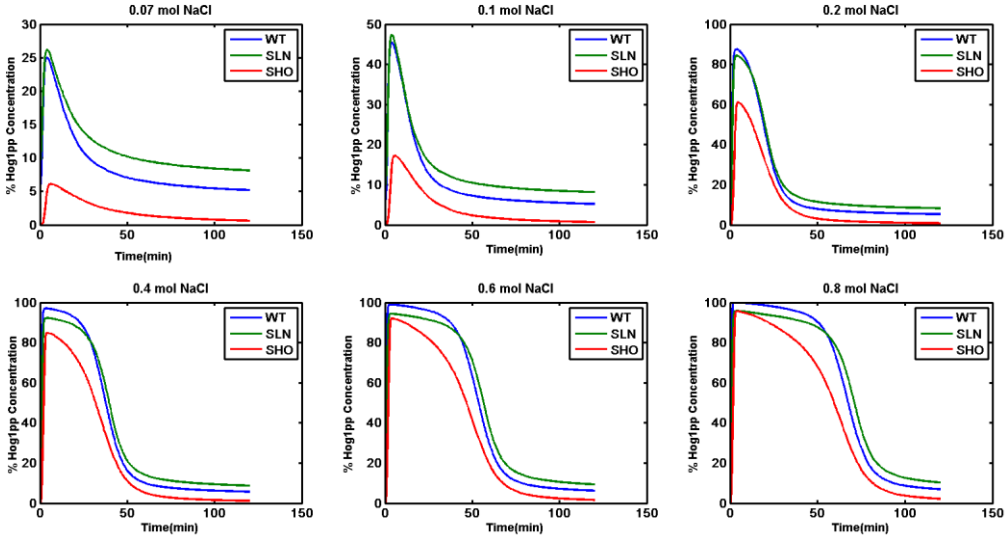

Figure 22: The behavior of the system with higher Pbs2pp dephosphorylation rates in a presentation similar to Figures 19 and 20.

Though possible, as demonstrated here, the scenario is purely hypothetical until further experimental data is available for the mechanism and kinetics of Pbs2pp dephosphorylation in the branches.

3.5 Information Flow in the System

One of the properties of a multi-branch biological system such as the HOG pathway is the information flow in the system. In the model created here, the input, that is the osmotic stress induced by a high NaCl concentration, is sensed by the sensors on the cell membrane and propagated through both branches to Hog1, which in turn induces glycerol production and accumulation. The glycerol accumulation elevates the internal pressure and brings about an equalization of internal and external pressure, a reduction in the input and adaptation of the system.

In order to investigate the information flow, the following approach was chosen:

- Since the information (the signal) is transmitted from one active species to the next, it was decided to only look at the active species (e.g. Ssk2p but not Ssk2).
- In order to quantify the information, for each species and for all stresses, the integral under the response curve was calculated (e.g. the integral of the curve of Sln1under 0.2 Mol NaCl). Since the concentration of all active species is rather low in a steady state, the integral of the base-line activity was not subtracted from the integral.
- In order to be able to compare the integrals of different species, they were normalized as the percentage relative to the maximum, that is the integral obtained for the highest stress (0.8 Mol NaCl).
- The same was done for the stress itself and is shown in all plots as a reference curve.

The integral of the signal curve does not have a physiological meaning per se but generally, higher osmotic stresses result in a longer time to adaptation and hence give rise to a larger integral. The advantage of the approach presented here is that the integral, a scalar, represents a whole curve and therefore allows a neat arrangement of the results for a number of species and all stresses on one plot.

The model is comprised of modules. It was decided to show the results for each module in one plot. Apart from the results for the species in the module, each plot contains the input of the module as well (e.g. the plot of the Pbs2 module contains the results for Ssk2p and Ste11p as well).

All plots contain as a reference the curve for the input – the NaCl concentrations.

3.5.1 Information Transmission in the Wild Type

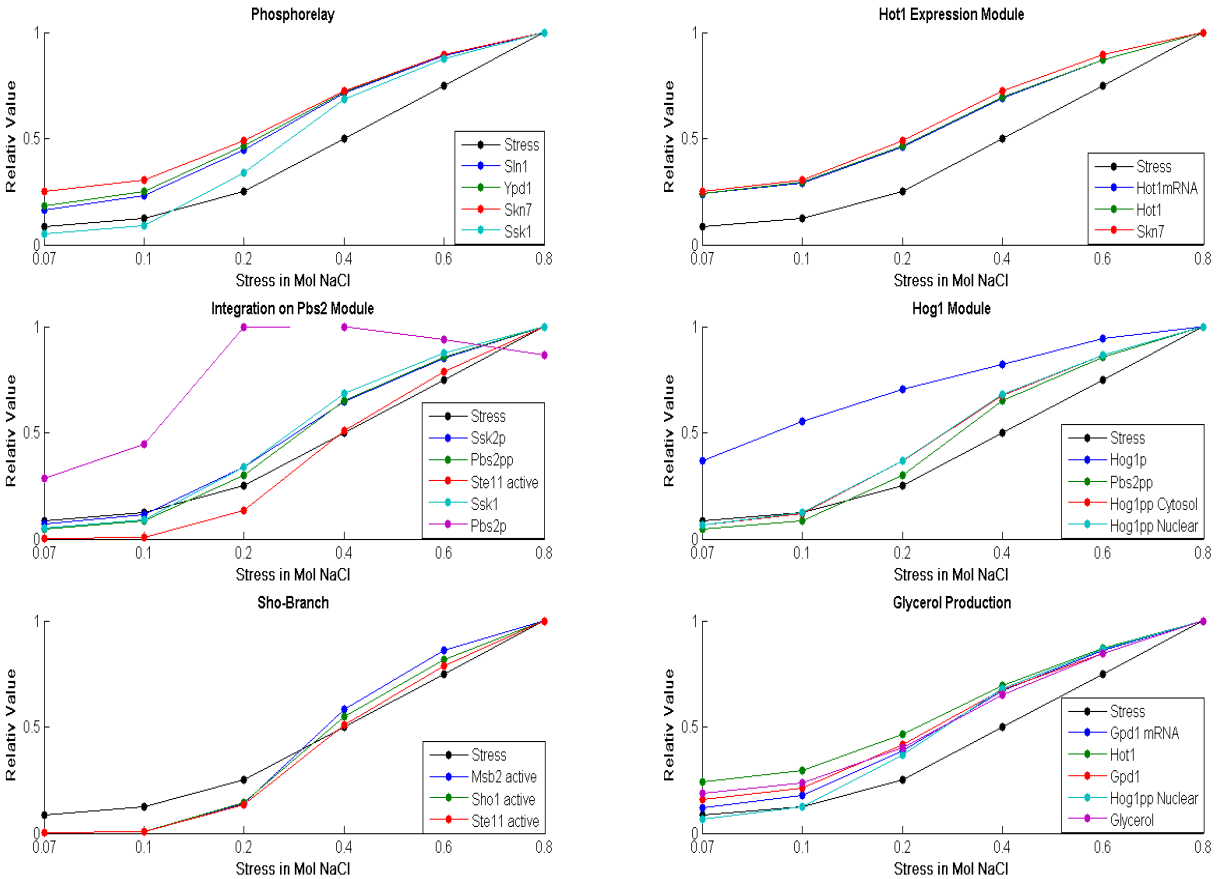

Figure 23: Species' integrals for the wild type strain. A dot represents an integral for a certain species under a certain stress.

3.5.1.1 Phosphorelay Module

- 0.07 – 0.1 Mol NaCl: For all species and stresses, the incline in integral size is parallel, meaning that the module responds proportionally to the increase in stress.
- 0.1 – 0.2 Mol NaCl: The incline for Sln1 is steeper than the stress, meaning that a twofold stress results in a more than twofold response for the furthest upstream element of the branch. Information transmission to Ypd1 is proprtional (parallel lines). Incline for Ssk1 is much steeper and for Skn7 a little less steep. Therefore the switch-like response of the branch occurs between 0.1 and 0.2 Mol NaCl. The exact value was determined to be 0.15 Mol NaCl.
- 0.2 – 0.4 Mol NaCl: Incline for all species but Ssk1 is parallel to stress
- 0.4 – 0.6 Mol NaCl: Incline for all species slightly less steep than for the stress

3.5.1.2 Hot1 Expression Module

From Skn7 to Hot1 mRNA, the transmission has a slightly less pronounced effect (incline of Skn7 steeper than incline for Hot1 mRNA). Information transmission between Hot1 and Hot1 mRNA is proportional.

3.5.1.3 Sho1 Branch Module

- 0.07 – 0.1 Mol NaCl: Stress incline is steeper than species incline.
- 0.1– 0.2 Mol NaCl: Inclines are all parallel
- 0.2 – 0.4 Mol NaCl: The incline for the species is steeper than for the stress. The jump occurs exactly at 0.22 Mol NaCl. Other than the results for the species of the phosphorelay module, the curves for the species here start to diverge. The information transmitted from one species to the next evokes a smaller integral. This can be interpreted as a slight weakening of the signal as opposed to an amplification of the signal in the Sln1 branch (via Ssk1 see 3.5.1.1).

3.5.1.4 Integration on Pbs2

Transmission from Ssk1 to Ssk2p is in general proportional (paralell lines) although a closer look will reveal that the curves cross each other at 0.2 Mol NaCl. The tranmission initially has an amplifing and then a weakening nature.

The transmission from Ssk2 tp Pbs2pp has a more similar incline than the incline of Ste11, as expected (wild type response is mainly determined by the Sln1 branch see…) .

Pbs2p has a different pattern than the other curves. However, Ssk2 and Pbs2pp have parallel curves, so that the intermediate species Pbs2p does not influence the overall transmission in the system. Lacking influence, Pbs2p might be superfluous in this model.

3.5.1.5 Hog1 Module

The cytosolic and nuclear Hog1pp have paralell inclines in integral size. The incline of Pbs2pp from 0.2 to 0.4 Mol NaCl is steeper than the incline for Hog1pp, suggesting a slight weakening of the signal between Pbs2pp and Hog1pp. Hog1p, as Pbs2p has a different incline pattern than other species in the module and its incline is less steep than the incline for both Pbs2pp and Hog1pp. Hog1p could be made accountable for the weakening of the signal between Pbs2pp and Hog1pp.

3.5.1.6 Glycerol Module

Though only slightly observable, the information transmission from nuclear Hog1pp to Gpd1 mRNA and to Gpd1 is convergent with a signal weakening nature. The curve for Gpd1 crosses the curve for glycerol at 0.16 Mol NaCl, and until 0.2 Mol NaCl there is a weakening transmission. From 0.2 Mol NaCl the curves are paralell and the information tranmission proportional. Interestingly, the glycerol curve is parallel to the Hot1 curve and not to the Hog1pp curve, although Hog1pp is the more important factor in glycerol production.

3.5.2 Information Transmission in the ΔSte11 Strain

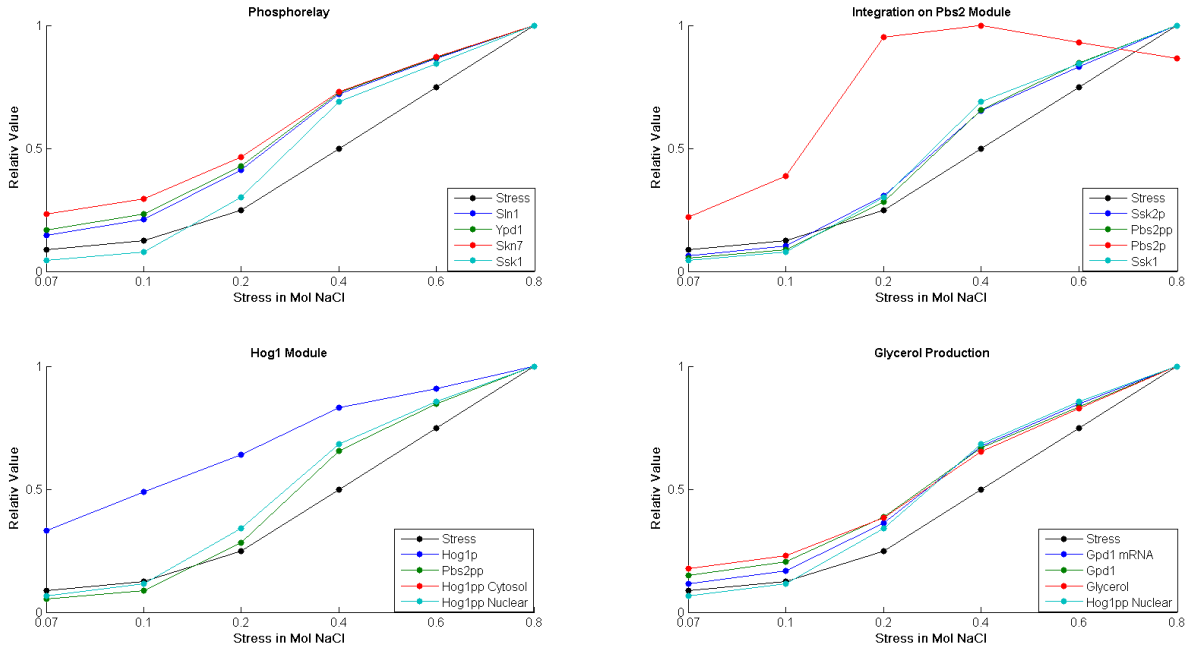

Figure 24: Species' integrals for the ΔSsk2 strain.

The information transmission here is not very different from the information transmission in the wild type. For the glycerol production module, the period in which the transmission between Gpd1 and glycerol has a slight weakening nature is shorter than in wild type. The curve for Gpd1 crosses the curve for glycerol at 0.19 Mol NaCl and (0.16 Mol for the wild type) and goes paralell to it at 0.2 Mol NaCl (like the wild type)

3.5.3 Information transmission in the ΔSsk2/ ΔSsk22 Strain

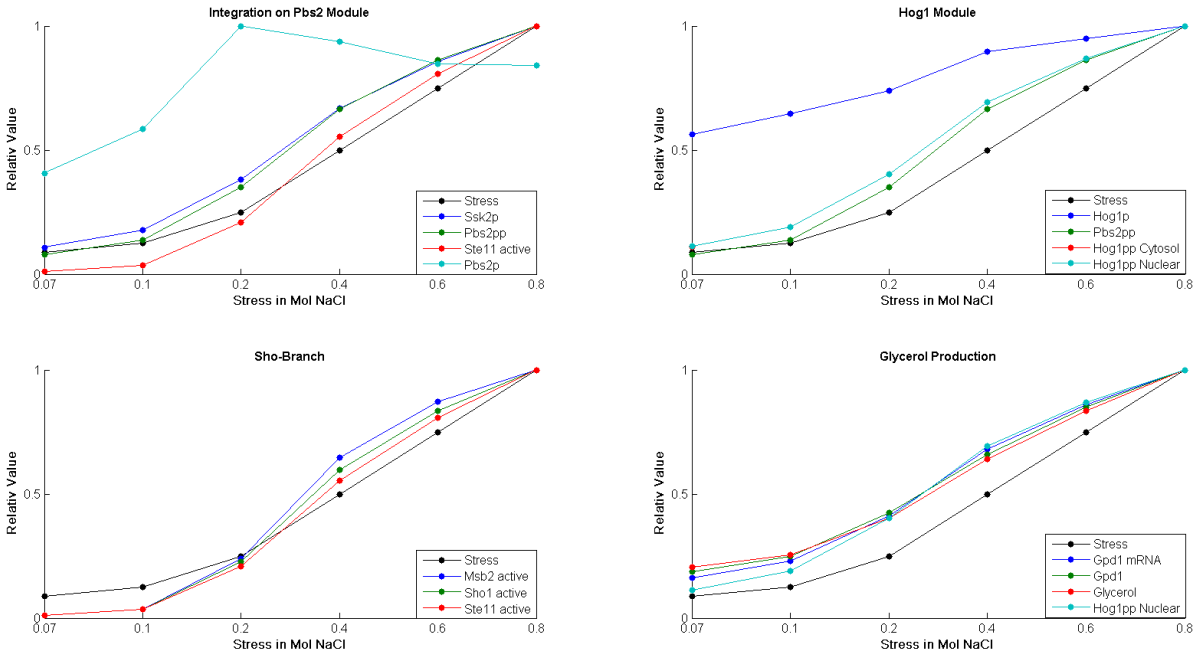

Figure 25: Species' integrals for the ΔSsk2/ΔSsk22 strain.

Here the weakening of the signal transmission in the Sho1 branch starts earlier than in the wild type (at 0.1 Mol NaCl instead of 0.2 Mol for the wild type). For the glycerol production module, the curves of Gpd1 and glycerol cross each other earlier than in the wild type or the ΔSte50 strain (0.12 Mol NaCl compared to 0.16 and 0.19 Mol in ΔSte50 strain and wild type, respectively).

3.6 Robustness and Sensitivity Analysis

Perturbation of initial species concentration and parameters is a tool used in mathematical modelling to show that the model is robust, and to identify and test features of the model that cannot be tested experimentally, as will be elaborated below.

3.6.1 Robustness

An adequate description of the experimental data by a model (see Chapter 3.1) and verification of its compliance with data from the literature (see Chapter 3.2) were the first steps in establishing the model's validity.

Species initial concentration values were taken from the literature, but as these concentrations were obtained experimentally, they might not be exact due to deviations in measurement devices, variant conditions of the cells themselves and all other problems and aspects of experimental work researchers encounter.

In experiments, overexpression of species included in the model resulted in viable cells, at least under normal environment conditions. It is therefore necessary to show that the model too is viable under normal conditions when initial species concentrations are varied.

Viability is regarded here as the capability of the model to reach a steady state under non-osmotic stress (that is when the NaCl concentration is 0 Mol).

As to null mutations, the literature shows that yeast cells cannot always cope with null mutations and become unviable. In this model it was already shown that some mutations upstream of Pbs2 result in the exclusion of one of the branches and are viable and responsive to osmotic stress as required by the experimental data of Macia *et al*. Null mutations downstream of Pbs2 might be viable in experiments but will not result in a functioning model.

The capability of the model to enter a steady state was tested with varying initial species concentrations (from 10% of the initial concentration to 1000% of it, for all species in the system).

As markers, seven species were chosen – Hog1pp, Ssk2, Sln1, Gpd1, Msb2, glycerol and cell volume. If the curves for these species become horizontal (or show a tendency to become horizontal) during the simulation, the model is regarded as robust to perturbation of the tested species.

Since the question addressed here is whether the curves for the markers are horizontal or not, the curves for the species were multiplied by a factor in a way that allows a neat arrangement of all seven markers on one plot.

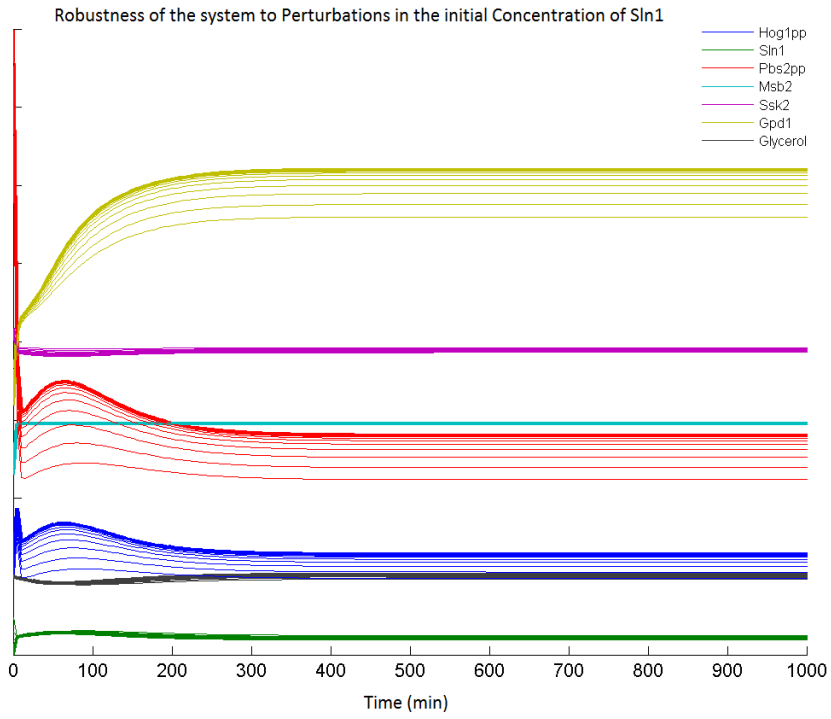

Figure 26: An example of the capability of species in the system to reach a steady state when initial concentrations are perturbed. 7 simulations are shown. In each simulation, the initial concentration of Sln1p is varied 10% and 1000% of the initial concentration.

For perturbation of Sln1 concentration, the model is capable of entering a steady state.

This was the case for all species (data not shown). However, the system takes longer to reach a steady state for some species.

Krantz *et al* [46] challenged the HOG pathway robustness experimentally by overexpressing the genes of its members and measuring the growth rate of cells with different overexpression profiles. Two genes were found to impair growth when overexpressed – Pbs2 and Ssk1. Krantz *et al* then examined the robustness of mathematical models. A measure for non-robustness of a model was defined as the accumulation of dual-phosphorylated Hog1 in the nucleus under steady state conditions (0 Mol NaCl). The model by Klipp *et al* was shown not to be robust against overexpression of Ssk1 and Ssk2, whereas overexpression of Pbs2 did not result in accumulation of nuclear Hog1pp and non-robustness.

This model shows the same results. A higher initial concentration of Ssk1 and Ssk2 results in a threefold accumulation of nuclear Hog1pp, whereas an increase of the initial concentrations of other species does not seem to effect nuclear Hog1pp accumulation.

3.6.2 Sensitivity

Once an adequate description of experimental data through mathematical modelling was achieved and the system was shown to exhibit robustness to perturbation of initial concentrations, the validity of the model is established.

A valid model makes it possible to perform a sensitivity analysis in order to examine properties of the models that are otherwise difficult or impossible to investigate experimentally.

Since the model describes the Macia data accurately it also enables a reliable comparison of the impact of the reactions on the system under varying stress conditions. In addition to the average sensitivity usually examined in theoretical works, the possibility that the system’s sensitivity to the parameters changes during the whole time span of the response is also examined, as will be elaborated below.

3.6.2.1 Sensitivity under Varying Stress conditions

First, in order to gain an approximate impression of the degree of sensitivity of the system and its species to all parameters, the average sensitivity over the whole time span was calculated according to the principles introduced in Section 2.2.10. Moreover, the possibility that different stress levels result in different sensitivities was tested as well.

The system under 0.1 Mol NaCl

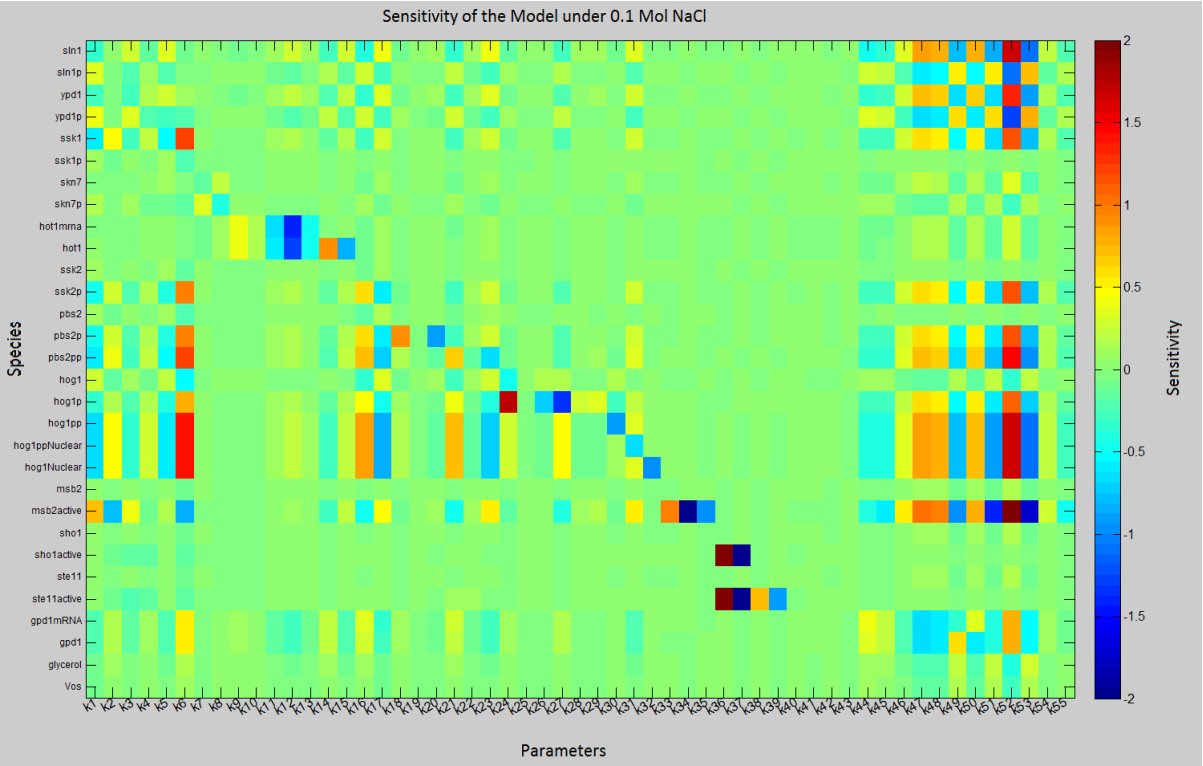

Figure 27: Sensitivity diagram for the all species and parameters under 0.1 Mol NaCl. Parameter index is attached as Annex…

Double phosphorylated Hog1, a measure for the system's behaviour, is most sensitive to (in descending order):

- The glycerol outflow rate
- The Vmax of channel closure
- Ssk1 dephosphorylation rate
- Glycerol formation rate
- Gpd1 formation rate
- The hill constant of Gpd1 mRNA
- Hog1pp nuclear transport
- Ssk2 activation and inactivation rates

As to the sensitivity of other species, Pbs2 and Hog1 species exhibit the highest sensitivity, followed by the phosphorelay species (in particular Ssk1). Active Msb2 is the only species in the Sho1 branch that shows sensitivity. Sensitivity is shown toward parameters of the glycerol production machinery (which prove highly

important in the model) followed by the parameters of the phosphorelay system, and Ssk2 reaction rates and Pbs2pp.

The system under 0.8 Mol NaCl

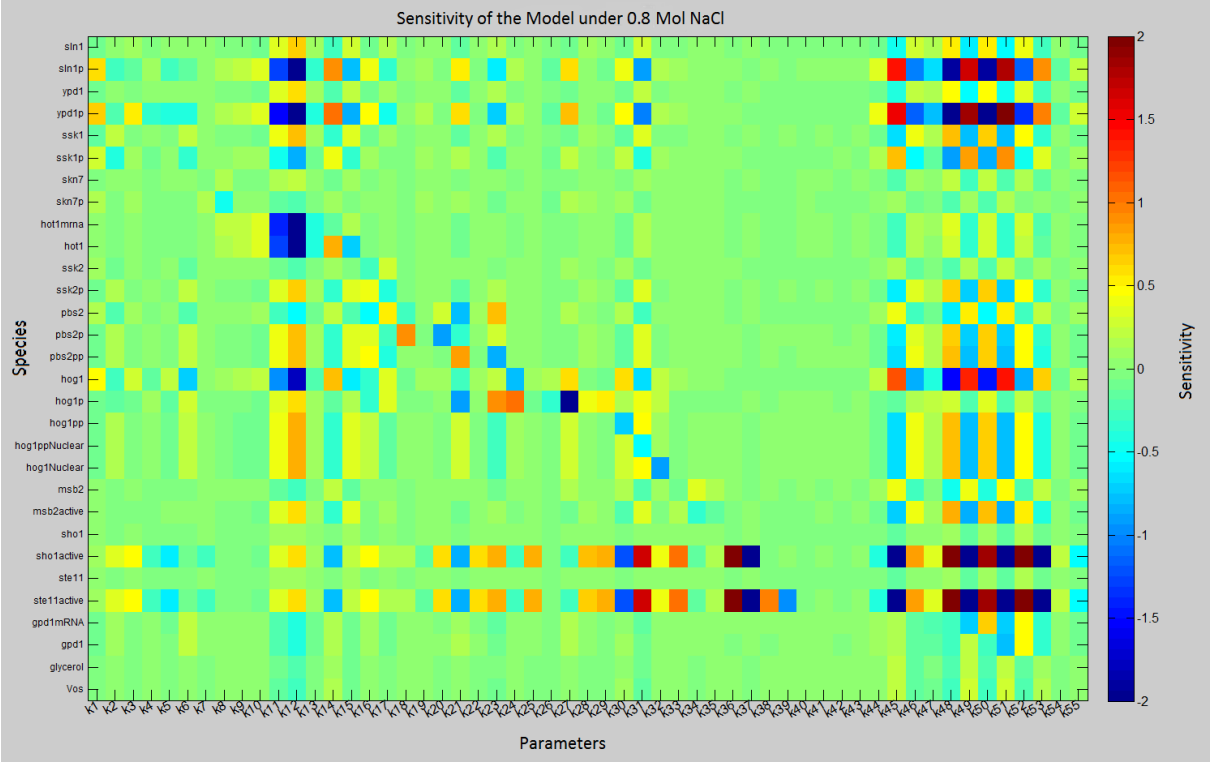

Fig 28 Sensitivity diagram for the all species and parameters under 0.8 Mol NaCl. Parameter index is attached in Annex 1.

Hog1pp is most sensitive to (in descending order):

- Gpd1 mRNA degradation rate
- Gpd1 formation and degradation rates
- Glycerol formation rate
- Hog1pp transport to nucleus and dephosphorylation rate
- Dissociation rate of Hot1 mRNA
- Hot1 degradation rate
- Vmax and degradation rate of Gpd1 mRNA

Species of the Sho1 branch become more sensitive under high osmotic stress. The channels still play an important role but not as important as in the case of 0.1 Mol NaCl. Under low osmotic stress, the pathway response is not as strong and

the cells rely on closure of the channels as a first response to the changes in their environment's osmolarity. For a higher stress, dephosphorylated Hog1 is more sensitive than the double phosphorylated form, probably due to depletion of Hog1 under high stress. The system here is still very sensitive to changes in the parameters of the glycerol production apparatus. The parameters of the Hot1 expression also play a more important role than under 0.1 Mol NaCl and the parameters of Ssk1 dephosphorylation and Ssk2 activation are less important. In general it can be concluded that under high osmotic stress the role of the channels becomes less important than the production of glycerol and the processes connected to it.

Sho1 vs. Sln1 branch

The existence of two branches that take part in osmo-sensing and response raised many questions among researchers as to what specific roles these branches might have. From a biological/evolutionary point of view, redundancy does not seem plausible due to the complexity of both branches. Hohmann [4] raised the hypothesis that the Sho1 branch might be more present when low stress is applied, whereas the Sln1 branch is more present under severe stress conditions.

An examination of the experimental data from Macia et al. does not support the hypothesis – the behaviour of the system under 0.07 and 0.1 Mol NaCl in the wild type is far more similar to the response of the ΔSte50 strain than to the response of the ΔSsk2/ ΔSsk22 strain. In both the wild type and ΔSte50 strain, the concentration of Hog1pp increases rapidly to 40% and 60% of the maximum in response to stresses of 0.07 and 0.1 Mol NaCl, respectively (Fig. 2-6), whereas the response in the ΔSsk2/ ΔSsk22 is quite different. Sensitivity analysis of the model supports what one sees with the naked eye – under 0.1 Mol NaCl the system is sensitive to the parameters of the Sln1 branch (especially to Ssk1 dephosphorylation rate) and insensitive to parameters of the Sho1 branch. Furthermore, under 0.8 Mol NaCl the species of the Sho1 branch are more sensitive to all parameters.

3.6.2.2. Sensitivity of the System in Different Response Phases

The system's response involves multiple phases, as indicated in the figure below:

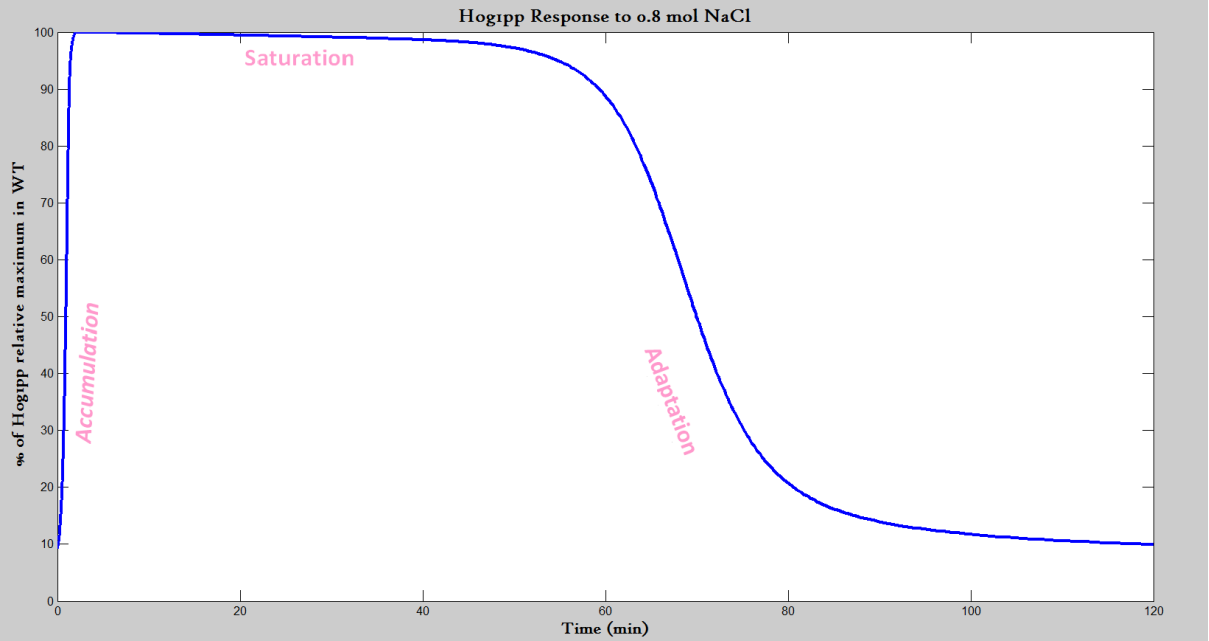

Fig 29: Time course for double phosphorylated Hog1 under 0.8 Mol NaCl

In the first phase, which lasts a few minutes, the HOG pathway responds to the stress and as a result Hog1 is double phosphorylated and enters the cell nucleus while the cell volume drops. In the second phase, Hog1pp reaches its maximum concentration and remains saturated while glycerol is being produced rapidly and the cell volume gains growth. In the third and last phase, the system adapts to the signal and the concentration of Hog1pp drops.

The system's goals change from phase to phase and therefore the behaviour of the species in the system must change with it. As a result, the sensitivity of the system to the reactions changes from one phase to the next. Such changes might not be detectable when performing a sensitivity analysis over the entire time span of the experiment, as was done in the last section.

For each phase, the average sensitivity over the time span of the phase was calculated for all species and parameters.

<u>Sensitivity in the Accumulation Phase</u>

In the accumulation phase, the branches are activated, Hog1pp accumulates and enters the nucleus.

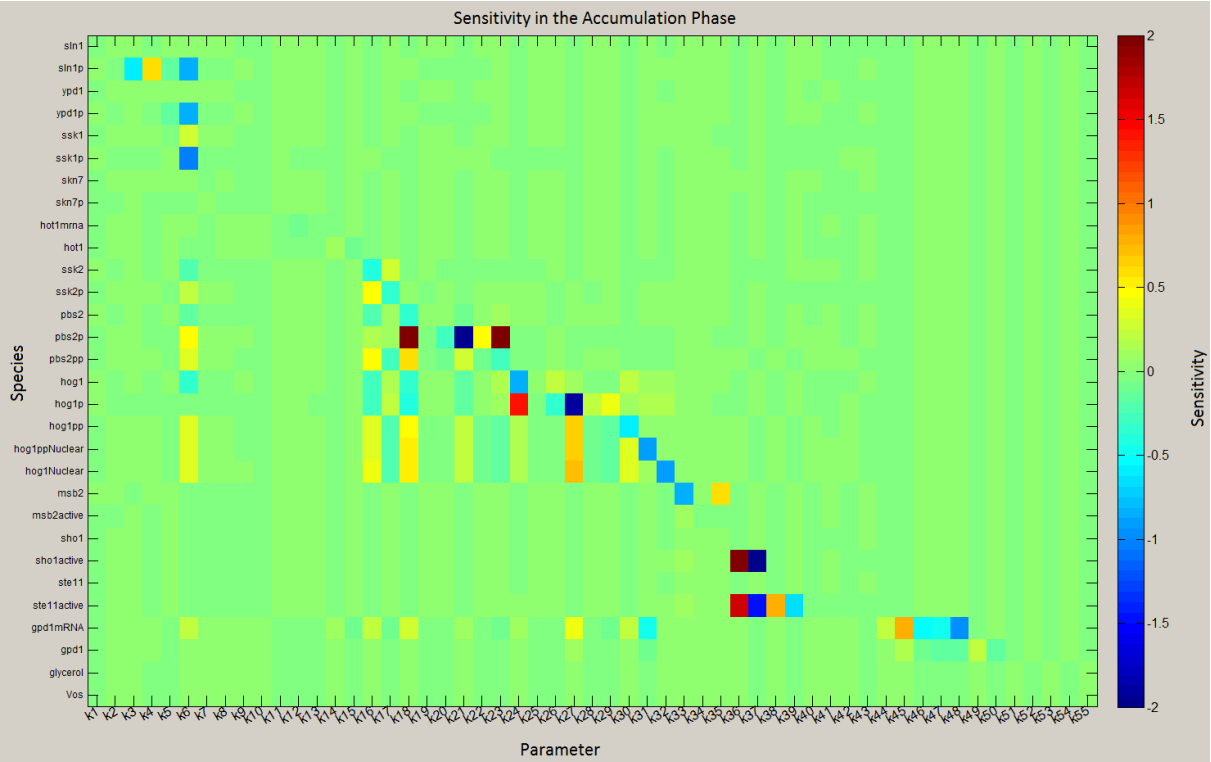

Figure 30: The average sensitivity for the accumulation phase

Hog1pp is most sensitive to its Vmax rate, the Vmax for Pbs2pp formation, Ssk1p dephosphorylation rate, the rates for the Hog1pp shuttle system and Ssk2 phosphorylation rate.

Although the system is generally more sensitive to the parameters of the input to the Sln1 branch than to Ssk1 dephosphorylation rate (see average sensitivity), this is not the case for the accumulation phase. Very little is needed to switch on the pathway, and the Ssk1 dephosphorylation rate and Vmax of Hog1pp are principally balanced by the shuttle system and Ssk2 dephosphorylation rate. In general, reaction in the system seem to be balanced by reactions that are part of other modules in the pathway.

As expected, the parameters of the glycerol production apparatus do not have an influence on the system during the accumulation phase. Although Gpd1 is also relatively inert in the accumulation phase, its mRNA is not – indicating that the cell is preparing itself for glycerol production.

Sensitivity in the Saturation Phase

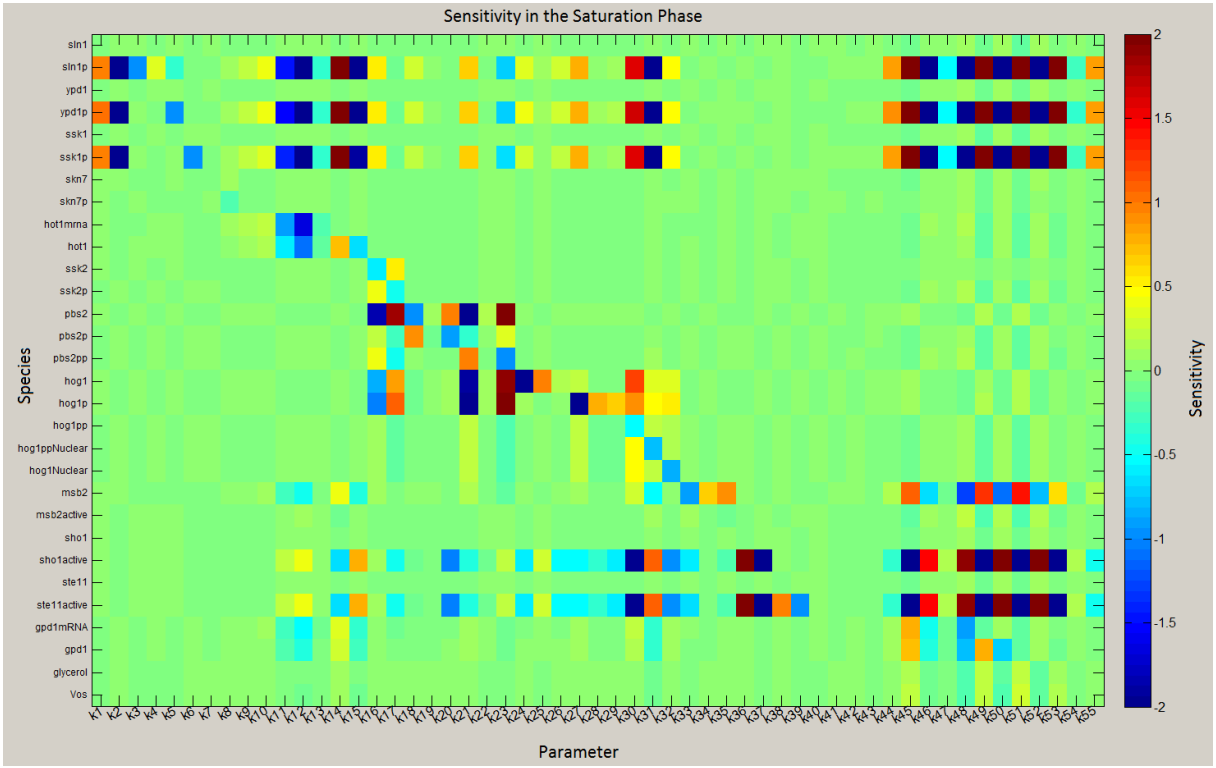

Figure 31: Sensitivity analysis in the saturation phase.

When saturated, Hog1pp is generally not very sensitive in comparison to the accumulation and adaptation phases. It is somewhat sensitive to the parameters of the shuttle system and the parameters of the Sln1 branch-related Pbs2 parameters. The branches become far more sensitive to their own parameters, the parameters of the glycerol apparatus and the Hot1 expression module. However, the parameters of the branches do not have any influence on other species in the model.

The species in the phosphorelay module and Sho1 branch are very sensitive in this phase. Interestingly, one can observe that the species within the branches are equally influenced by the system's parameters, thereby showing a proportional information transmission from one species to the next.

Sensitivity in the Adaptation Phase

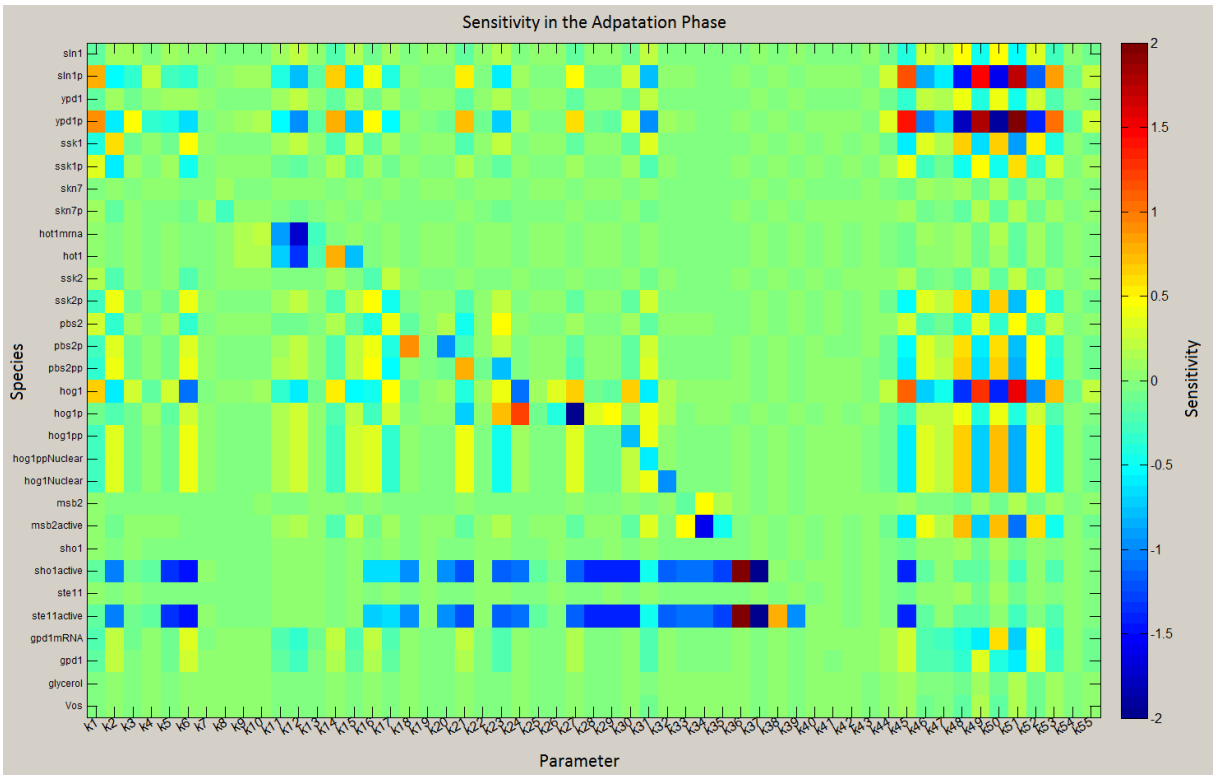

Figure 32: Sensitivity in the adaptation phase

In the adaptation phase, Hog1 species are more sensitive to parameters of the glycerol production machinery. The parameters of Hot1 expression have a lesser influence than in the saturation phase. The parameters of the phosphorelay system become more influential.

Whereas the information transmission between Sho1 and Ste11 stays proportional, this transmission in the Sln1 branch is not.

4. Summary

The model presented here is used to investigate various aspects of the yeast's osmoadaptation. The model is comprised of two branches – the Sln1 branch and the Sho1 branch which sense the biophysical changes that the yeast cell undergoes when osmotic shock is applied, Pbs2 - the furthest downstream element of the two branches which initiates the dual phosphorylation of Hog1, Hog1 - that when dual phosphorylated, enters the cell nucleus and activates the glycerol production apparatus, and glycerol - which accumulates upon both this

production and a reduction of its outflow from the cell due to channel closure. Accumulation of glycerol raises the intracellular osmolarity, thereby balancing the high extracellular osmolarity. This leads to a reduction of the input's strength and to adaptation of the system. An additional feed-forward loop in the system is hypothesized and implemented as a regulation of Hot1 – a transcription factor that is known to play a role, together with Hog1, in the regulation of glycerol producing enzymes. It was hypothesized that Hot1 regulation is carried out by Skn7, a transcription factor that has been shown to be a part of the phosphorelay system and to interact with Hot1.

Experimental data for three strains (the wild type, ΔSte11 strain and ΔSsk2/ ΔSsk22 strain), under different degrees of osmotic stress was obtained by Macia *et al* [3]. This data is described adequately by the model. The most significant shortcoming of the model, in regard to the experimental data, is the response of the wild type and the ΔSte11 strain to weak osmotic stress. The experimental data shows a much faster adaptation to these conditions. Macia created a simple model that describes rapid adaptation to low osmotic stress adequately. However, it contains an internal negative feedback of dual-phosphorylated Hog1 on its own phosphorylation. Such a negative feedback, that might be accountable to the rapid adaptation, was not modelled here. Nevertheless, this rapid adaptation to weak stresses was not shown in other experiments, such as those shown in Zhike *et al* [2].

Another shortcoming of the model is the adaptation to the strongest stress (0.8 Mol NaCl), which occurs too fast in the model. A simulation of the model without the transcription factor Skn7, which is hypothesized to play a role in a feed-forward loop, appears to show a better adaptation under strong stresses.

Sensing osmotic stress by the Sho1 branch is elusive. In this work it was modeled in dependency of the turgor pressure, similar to the input for the Sln1 branch. Other publications have suggested a different sensing mechanism, such as direct sensing of the extracellular osmolite concentration, or sensing the intracellular pressure or changes in the cell volume. These various possibilities are discussed in the work. Intracellular biophysical properties such as volume change, turgor pressure and internal pressure are all dependent on each other and therefore one would expect that modelling the sensing in dependency of one of these factors

would be possible, with a few modifications and fine tuning of the parameters. The work demonstrates that this is indeed the case.

In order to reinforce the validity of the model it was shown to be in line with experimental results from other publications, such as Klipp [1], Muzzey [32] and Rep [28].

One of the scopes of this model was to explore the possibility of a feed-forward loop in the HOG pathway. A hypothesis of gene expression regulation of Hot1 by Skn7, which would result in fine regulation of Gpd1 expression, was considered, because the literature contains supporting evidence for the involvement of Skn7 in the phosphorelay system, the role of Hot1 in Gpd1 expression, and a possible nexus between Skn7 and Hot1.

Mettetal *et al* [37] have suggested that mRNA species might play a role in the adaptation to a scenario in which the yeast is subject to consecutive stress pulses. They showed that adaptation is more effective if mRNA translation apparatus is present in the cell and less effective if this apparatus is absent. As the model contains two mRNA species, the question of which specie is more likely to account for the effect, is discussed thoroughly. A simulation was designed in order to mimic the scenario of consecutive stress pulses accurately. A similar effect to that shown in the Mettetal publication could be observed.

One of the less investigated aspects of the HOG pathway is the convergence of the signal from the Sln1 and Sho1 branches to Pbs2. This aspect is discussed in this work. Macia's experiments suggest that the branches do not contribute equally to the response in the wild type. The Sln1 branch seems to be far more dominant than the Sho1 branch. Parmar *et al* [10] suggested in their model that this dominance is due to negative feedback in the Sho1 branch, carried out by the dual-phosphorylated Hog1 itself. This may not be in line with the experimental data of Macia, in which both ΔSte11 strain and ΔSsk2/ ΔSsk22 strain are capable of responding and adapting to an osmotic shock. Here a different hypothesis is suggested. It involves the dephosphorylation rates of the two forms of Pbs2: the MAPKK, Sln1 branch-related form, and the scaffold protein, Sho1 branch-related form. Nbp2 is known to participate in the inactivation of the protein scaffold in the Sho1 branch, to which Pbs2 belongs. The small quantity of Nbp2 molecules in

comparison to Pbs2 molecules could make this a limiting factor for Pbs2 dephosphorylation. As a result, different dephosphorylation profiles for the wild type, ΔSte11 strain and ΔSsk2/ ΔSsk22 strain might exist, as is discussed widely in the work. A simulation with a different dephosphorylation profile resulted in a greater similarity between the response of the wild type and that of the ΔSte11 strain. Apart from the information regarding Nbp2 very little is known about the dephosphorylation of dual-phosphorylated Pbs2. Further data is needed in order to investigate the convergence of both branches on the level of Pbs2.

Information transmission in the system was examined by using the integral under the response curves of all active species, for all strains, and under all stress degrees as a measure.

It was found that information transmission in the Sln1 branch differs from information transmission in the Sho1 branch. The precise amount of stress needed to activate the branches in a switch-like manner was determined, and effects such as parallel, amplifying and weakening transmission were discussed. The contribution of intermediate species such as single phosphorylated Pbs2 and Hot1 was discussed as well.

In order to further establish the validity of the model, the robustness of the model was challenged. The ability of the model to reach a steady state was considered as a measure for the robustness. Experimental data by Kranz *et al* [46] showed that the yeast has a growth defect when Pbs2 and Ssk1 are overexpressed. They suggested a different measure for robustness in mathematical models, namely that the cell would be deemed robust to perturbations if they will not lead to accumulation of dual-phosphorylated Hog1 in the nucleus under 0 Mol NaCl. Ssk1 and Ssk2 were found to induce accumulation of dual-phosphorylated Hog1 in the nucleus when overexpressed. The model did not reproduce the non-robustness of the cell to overexpression of Pbs2.

A valid mathematical model, such as the one presented here, enables the researcher to conduct a sensitivity analysis and make reliable statements regarding the behaviour of the living cell. The sensitivity of the model under 0.1 Mol NaCl was compared to the sensitivity under 0.8 Mol NaCl. Many differences were found and described. For example, under 0.1 Mol NaCl, the system is more

sensitive to perturbations in the parameters of the channel system than to those of glycerol production. Under 0.8 Mol NaCl, the situation is reversed. Under both 0.1 and 0.8 Mol NaCl the system is not sensitive to perturbations of the parameters of the Sho1 branch, but species in the Sho1 branch become sensitive to perturbations under 0.8 Mol NaCl.

The system's response can be divided into three phases – the accumulation, saturation and adaptation phases. It was decided to conduct a sensitivity analysis for the three phases separately. Some interesting and surprising observations were made. For instance, the parameters for the input of the branches become important in the adaptation phase, whereas in the accumulation phase parameters of species in the middle of the Sln1 branch, such as Ssk1 and Ssk2 parameters, seem to be more important. The importance of a parameter, for example the phosphorylation rate of species, does not automatically mean that the parameters for dephosphorylation of those species have the same degree of importance.

The valid model created in this work can be used for further investigations of other properties of the HOG pathway. It can be extended to include other features of the pathway, integrated into other models of different processes in the yeast, or be used as a platform for integrating additional models. As such, the model could contribute to our understanding of the amazing biology of yeast.

Acknowledgements

I would like to thank Prof. Dr. Dr. h.c. Edda Klipp and Prof. Dr. Andreas Möglich for the supervision and assessment of my master thesis.

Special thanks to Christian Waltermann for his time, support, advice and assistance in all aspects of this work.

References

1. Edda Klipp, Bodil Nordlander, Roland Krüger, Peter Gennemark & Stefan Hohmann. **Integrative model of the response of yeast to osmotic shock**. ***Nature Biotechnology*** 23, 975 - 982 (2005)

2. Zhike Zi, Wolfram Liebermeister, Edda Klipp (2010). **A Quantitative Study of the Hog1 MAPK Response to Fluctuating Osmotic Stress in Saccharomyces cerevisiae**. *PLoS ONE 5(3): e9522. doi:10.1371/journal.pone.0009522*

3. Javier Macia, Sergi Regot, Tom Peeters, Núria Conde, Ricard Solé and Francesc Posas. Dynamic Signaling in the Hog1 MAPK Pathway Relies on High Basal Signal Transduction(2009). *Science Signaling 2 (63), ra13*

4. Stefan Hohmann. **Osmotic Stress Signaling and Osmoadaptation in Yeasts.** *MICROBIOLOGY AND MOLECULAR BIOLOGY REVIEWS, June 2002, p. 300–372*

5. Fabiola Janiak-Spens, Paul F. Cook, and Ann H. West. **Kinetic Analysis of YPD1-Dependent Phosphotransfer Reactions in the Yeast Osmoregulatory Phosphorelay System**. *Biochemistry 2005, 44, 377-386*

6. Posas F, Wurgler-Murphy SM, Maeda T, Witten EA, Thai TC, Saito H. **Yeast HOG1 MAP kinase cascade is regulated by a multistep phosphorelay mechanism in the SLN1-YPD1-SSK1 "two-component" osmosensor**. *Cell 86(6):865-75*

7. Kazuo Tatebayashi, Keiichiro Tanaka, Hui-Yu Yang, Katsuyoshi Yamamoto, Yusaku Matsushita, Taichiro Tomida, Midori Imai and Haruo Saito. **Transmembrane mucins Hkr1 and Msb2 are putative osmosensors in the SHO1 branch of yeast HOG pathway**. *EMBO J26(15):3521-33*

8. Wu C, Jansen G, Zhang J, Thomas DY, Whiteway M (2006) **Adaptor protein Ste50p links the Ste11p MEKK to the HOG pathway through plasma membrane association**. ***Genes Dev 20****: 734–746*

9. Reiser V, Raitt DC, Saito H. **Yeast osmosensor Sln1 and plant cytokinin receptor Cre1 respond to changes in turgor pressure**. *J Cell Biol 161(6):1035-40*

10. J H Parmar, Sharad Bhartiya and K V Venkatesh. **A model-based study delineating the roles of the two signaling branches of Saccharomyces cerevisiae, Sho1 and Sln1, during adaptation to osmotic stress.** *Phys. Biol. 6 (2009) 036019 (13pp).*

11. Janiak-Spens F, West AH**. Functional roles of conserved amino acid residues surrounding the phosphorylatable histidine of the yeast phosphorelay protein YPD1.** *Mol Microbiol. 2000 Jul;37(1):136-44.*

12. Chang C, Meyerowitz EM. **Eukaryotes have "two-component" signal transducers.** *Res Microbiol. 1994 Jun-Aug;145(5-6):481-6. Review.*

13. **Posas** F, Saito H. **Activation of the yeast SSK2 MAP kinase kinase kinase by the SSK1 two-component response regulator.** *EMBO J. 1998 Mar 2;17(5):1385-94.*

14. Keener, J.; Sneyd, J. **Mathematical Physiology: I: Cellular Physiology (2 ed.).** *Springer (2008).*

15. Posas F and Saito H. **Osmotic activation of the HOG MAPK pathway via Ste11p MAPKKK: scaffold role of Pbs2p MAPKK**. *Science 276(5319):1702-5 (1997).*

16. O'Rourke SM and Herskowitz I. **Unique and redundant roles for HOG MAPK pathway components as revealed by whole-genome expression analysis**. *Mol Biol Cell 15(2):532-42 (2004).*

17. Cullen PJ, Sabbagh W Jr, Graham E, Irick MM, van Olden EK, Neal C, Delrow J, Bardwell L, Sprague GF Jr**. A signaling mucin at the head of the Cdc42- and MAPK-dependent filamentous growth pathway in yeast.** *Genes Dev 18(14):1695-708 (2004).*

18. Krems B, *et al*. **The response regulator-like protein Pos9/Skn7 of Saccharomyces cerevisiae is involved in oxidative stress resistance**. *Curr Genet29(4):327-34 (1996)***.**

19. Ikner A and Shiozaki K. **Yeast signaling pathways in the oxidative stress response**. *Mutat Res 569(1-2):13-27 (2005).*

20. Rep M, Reiser V, Gartner U, Thevelein JM, Hohmann S, Ammerer G, Ruis H. **Osmotic stress-induced gene expression in Saccharomyces cerevisiae requires Msn1p and the novel nuclear factor Hot1p**. *Mol Cell Biol. (1999)*

21. Alepuz PM, de Nadal E, Zapater M, Ammerer G, Posas F. **Osmostress-induced transcription by Hot1 depends on a Hog1-mediated recruitment of the RNA Pol II.** *EMBO J. 2003 May 15;22(10):2433-42.*

22. Morgan BA, Banks GR, Toone WM, Raitt D, Kuge S, Johnston LH. **The** Skn7 response regulator controls gene expression **in the** oxidative stress response **of the** budding yeast Saccharomyces cerevisiae**.** *EMBO J. 1997 Mar 3;16(5):1035-44.*

23. **S**hiozaki K and Russell P. **Counteractive roles of protein phosphatase 2C (PP2C) and a MAP kinase kinase homolog in the osmoregulation of fission yeast.** *EMBO J 14(3):492-502 (1995)*

24. *Brewster JL, de Valoir T, Dwyer ND, Winter E, Gustin MC.**An osmosensing signal transduction pathway in yeast**. Science 259(5102):1760-3 (1993)*

25. Westfall PJ, Ballon DR, Thorner J. **An osmosensing signal transduction pathway in yeast**. *Science. 2004 Nov 26;306(5701):1511-2*

26. Tamás MJ, Luyten K, Sutherland FC, Hernandez A, Albertyn J, Valadi H, Li H, Prior BA, Kilian SG, Ramos J, Gustafsson L, Thevelein JM, Hohmann S. **Fps1p controls the accumulation and release of the compatible solute glycerol in yeast osmoregulation**. *Mol Microbiol. 1999 Feb;31(4):1087-104.*

27. Luyten K, Albertyn J, Skibbe WF, Prior BA, Ramos J, Thevelein JM, Hohmann S. **Fps1, a yeast member of the MIP family of channel proteins, is a facilitator for glycerol uptake and efflux and is inactive under osmotic stress**. *EMBO J. 1995 Apr 3;14(7):1360-71.*

28. Rep M, Krantz M, Thevelein JM, Hohmann S. **The transcriptional response of Saccharomyces cerevisiae to osmotic shock. Hot1p and Msn2p/Msn4p are required for the induction of subsets of high osmolarity glycerol pathway-dependent genes**. *J Biol Chem. 2000 Mar 24;275(12):8290-300.*

29. Albertyn J, Hohmann S, Thevelein JM, Prior BA. **GPD1, which encodes glycerol-3-phosphate dehydrogenase, is essential for growth under osmotic stress in Saccharomyces cerevisiae, and its expression is regulated by the high-osmolarity glycerol response pathway.** *Mol Cell Biol. 1994 Jun;14(6):4135-44.*

30. Edda Klipp, Wolfram Liebermeister, Christoph Wierling, Axel Kowald, Hans Lehrach, and Ralf Herwig. **Systems Biology: A Text Book.** *Wiley-VCH Verlag GmbH & Co. KGaA (24. Juni 2009)*

31. Hayles B, Yellaboina S, Wang D (2010) **Comparing Transcription Rate and mRNA Abundance as Parameters for Biochemical Pathway and Network Analysis.** *PLoS ONE 5(3): e9908. doi:10.1371/journal.pone.0009908*

32. Dale Muzzey,Carlos A. Gomez-Uribe, Jerome T. Mettetal, and Alexander van Oudenaarden. **A systems-level analysis of perfect adaptation in yeast osmoregulation.** *Cell. 2009 Jul 10;138(1):160-71.*

33. Wysocki R, Chéry CC, Wawrzycka D, Van Hulle M, Cornelis R, Thevelein JM, Tamás MJ. **The glycerol channel Fps1p mediates the uptake of arsenite and antimonite in Saccharomyces cerevisiae.** *Mol Microbiol. 2001 Jun;40(6):1391-401.*

34. Mollapour M, Piper PW. **Hog1 mitogen-activated protein kinase phosphorylation targets the yeast Fps1 aquaglyceroporin for endocytosis, thereby rendering cells resistant to acetic acid.** *Mol Cell Biol. 2007 Sep;27(18):6446-56. Epub 2007 Jul 9.*

35. Pfeuty B, Kaneko K. **The combination of positive and negative feedback loops confers exquisite flexibility to biochemical switches.** *Phys Biol. 2009 Nov 12;6(4):046013.*

36. Alon U. **Network motifs: theory and experimental approaches.** *Nat Rev Genet. 2007 Jun;8(6):450-61.*

37. Mettetal JT, Muzzey D, Gómez-Uribe C, van Oudenaarden A. **The frequency dependence of osmo-adaptation in Saccharomyces cerevisiae.** *Science. 2008 Jan 25;319(5862):482-4.*

38. Narsai R, Howell KA, Millar AH, O'Toole N, Small I, Whelan J. **Genome-wide analysis of mRNA decay rates and their determinants in Arabidopsis thaliana.** *Plant Cell. 2007 Nov;19(11):3418-36. Epub 2007 Nov 16.*

39. Michnick S, *et al.* **Modulation of glycerol and ethanol yields during alcoholic fermentation in Saccharomyces cerevisiae strains overexpressed or disrupted for GPD1 encoding glycerol 3-phosphate dehydrogenase.** *Yeast (1997) 13(9):783-93*

40. Alepuz PM, Jovanovic A, Reiser V, Ammerer G **Stress-induced map kinase Hog1 is part of transcription activation complexes.** *Mol Cell. 2001 Apr;7(4):767-77.*

41. Giaever G, et al. **Functional profiling of the Saccharomyces cerevisiae genome.** *Nature 2002 418(6896):387-91*

42. Tatebayashi K, Takekawa M, Saito H **A docking site determining specificity of Pbs2 MAPKK for Ssk2/Ssk22 MAPKKKs in the yeast HOG pathway.** *EMBO J. 2003 Jul 15;22(14):3624-34.*

43. Schwartz MA, Madhani HD. **Principles of MAP kinase signaling specificity in Saccharomyces cerevisiae.** *Annu Rev Genet. 2004;38:725-48.*

44. Malleshaiah MK, Shahrezaei V, Swain PS, Michnick SW. **The scaffold protein Ste5 directly controls a switch-like mating decision in yeast.** *Nature. 2010 May 6;465(7294):101-5. Epub 2010 Apr 18.*

45. Mapes J, Ota IM. **Nbp2 targets the Ptc1-type 2C Ser/Thr phosphatase to the HOG MAPK pathway.** *EMBO J. 2004 Jan 28;23(2):302-11. Epub 2003 Dec 18.*

46. Krantz M, Ahmadpour D, Ottosson LG, Warringer J, Waltermann C, Nordlander B, Klipp E, Blomberg A, Hohmann S, Kitano H. **Robustness and fragility in the yeast high osmolarity glycerol (HOG) signal-transduction pathway.** *Mol Syst Biol. 2009;5:281. Epub 2009 Jun 16.*

Annex 1: Equations, Initial Species' Concentrations and Parameters

Equations, Initial Species' Concentrations and parameters were partially adopted from Klipp et al 2005 and Zhike et al 2010.

Equation: For some of the reactions different kinetics were chosen.

Initial concentrations: Total numbers of molecules per specie were taken from www.yeastgenome.org. The concentrations were calculated in respect to cell volume of 58 fL. Concentrations of non-phosphorylated, one-fold phosphorylated and dual-phosphorylated forms were estimated under the assumption that concentrations of inactive forms are higher. Steady state simulations were run before running simulations under osmotic stress conditions.

Parameters: Unknown parameters were found during model development while taking into consideration common principles and data from the literature.

Phosphorelay Module and Ssk2

$$InputSln1(t) = k1 \cdot \frac{turgor\,(t)}{turgor_{(t=0)}}^{k2}$$

$$\frac{d}{dt} Sln1 = -InputSln(t) \cdot Sln1 + k3 \cdot Sln1p \cdot Ypd1 - k4 \cdot Sln1 \cdot Ypd1p - Sln1 \cdot V_r$$

$$\frac{d}{dt} Sln1p = InputSln(t) \cdot Sln1 - k3 \cdot Sln1p \cdot Ypd1 + k4 \cdot Sln1 \cdot Ypd1p - Sln1 \cdot V_r$$

$$\frac{d}{dt} Ypd1 = k5 \cdot Ssk1 \cdot Ypd1p - k3 \cdot Sln1p \cdot Ypd1 + k4 \cdot Sln1 \cdot Ypd1p + k7 \cdot Skn7 \cdot Ypd1p - Ypd1 \cdot V_r$$

$$\frac{d}{dt} Ypd1p = k3 \cdot Sln1p \cdot Ypd1 - k5 \cdot Ssk1 \cdot Ypd1p - k4 \cdot Sln1 \cdot Ypd1p - k7 \cdot Skn7 \cdot Ypd1p - Ypd1p \cdot V_r$$

$$\frac{d}{dt} Ssk1 = k6 \cdot Ssk1p - k5 \cdot Ssk1 \cdot Ypd1p - Ssk1 \cdot V_r$$

$$\frac{d}{dt} Ssk1p = k5 \cdot Ssk1 \cdot Ypd1p - k6 \cdot Ssk1p - Ssk1p \cdot V_r$$

$$\frac{d}{dt} Skn7 = k8 \cdot Skn7p - k7 \cdot Skn7 \cdot Ypd1p - Skn7 \cdot V_r$$

$$\frac{d}{dt} Skn7p = k7 \cdot Skn7 \cdot Ypd1p - k8 \cdot Skn7p - Skn7 \cdot V_r$$

$$\frac{d}{dt} Ssk2 = k17 \cdot Ssk2p - k16 \cdot Ssk1 \cdot Ssk2 - Ssk2 \cdot V_r$$

$$\frac{d}{dt}\,Ssk2p = k16 \cdot Ssk1 \cdot Ssk2 - k17 \cdot Ssk2p - Ssk2p \cdot V_r$$

Concentrations: Sln1 =0.016 µM Ypd1 =0.156 µM Ssk1 =0.029 µM Skn7 =0.4362 µM Ssk2 =0.00521 µM

k1 = 2.5 min^{-1}	A factor for the input equation for the Sln1 branch
k2 = 4	A coefficient for the input equation for the Sln1 branch (dimensionless)
k3 = 50 $(\mu M \cdot min)^{-1}$	Ypd1 phosphorylation rate
k4 = 50 $(\mu M \cdot min)^{-1}$	Ypd1p dephosphorylation rate
k5 = 50 $(\mu M \cdot min)^{-1}$	Ssk1 phosphorylation rate
k6 = 0.415 min^{-1}	Ssk1p dephosphorylation rate
k7 = 0.003 $(\mu M \cdot min)^{-1}$	Skn7 phosphorylation rate
k8 = 0.005 min^{-1}	Skn7p dephosphorylation rate
k16 = 2.3070 $(\mu M \cdot min)^{-1}$	Ssk2 activation rate
k17 = 0.07 min^{-1}	Ssk2p inactivation rate

Hot1 Expression Module

$$\frac{d}{dt}\,Hot1mRNA = k9 + k10 \cdot \frac{(Skn7/k11)^{k12}}{1 + (Skn7/k11)^{k12}} - k13 \cdot Hot1mRNA - Hot1mRNA \cdot V_r$$

$$\frac{d}{dt}\,Hot1 = k14 \cdot Hot1mRNA - k15 \cdot Hot1 - Hot1 \cdot V_r$$

Concentrations: Hot1 mRNA = 0.0001 µM (rough estimation) Hot1 = 0.0256 µM

k9 = 0.000007 min^{-1}	Basal transcription level of Hot1mRNA
k10 = 0.018 min^{-1}	Maximal rate of the formation of Hot1mRNA
k11 = 2.7 µM	Dissociation constant of the formation of Hot1mRNA
k12 = 4	Hill coefficient for the formation of Hot1mRNA
k13 = 0.0006 min^{-1}	Hot1mRNA degradation rate
k14 = 0.04 min^{-1}	Formation rate of Hot1
k15 = 0.0042 min^{-1}	Degradation rate of Hot1

Sho1 Branch

$$InputSho1(t) = k33 \cdot (1 - \frac{turgor\,(t)}{turgor_{(t=0)}})^{k34}$$

$$\frac{d}{dt}\,Msb2 = -InputSho1(t) \cdot Msb2 + k35 \cdot Msb2active - Msb2 \cdot V_r$$

$$\frac{d}{dt} Msb2 = Input\mathbf{Sho1}(t) \cdot Msb2 - k35 \cdot Msb2active - Msb2active \cdot V_r$$

$$\frac{d}{dt} Sho1 = -k36 \cdot Msb2active \cdot Sho1 + k37 \cdot Sho1p - Sho1 \cdot V_r$$

$$\frac{d}{dt} Sho1p = k37 \cdot Sho1p - k36 \cdot Msb2active \cdot Sho1 - Sho1p \cdot V_r$$

$$\frac{d}{dt} Ste11 = -k38 \cdot Sho1p \cdot Ste11 + k39 \cdot Ste11p - Ste11 \cdot V_r$$

$$\frac{d}{dt} Ste11p = k39 \cdot Ste11p - k38 \cdot Sho1p \cdot Ste11 - Ste11p \cdot V_r$$

Concentrations: Msb2 = 0.0315 µM Sho1 = 0.0556 µM Ste11 = 0.0178

k33 = 1.125 min^{-1}	A factor for the input equation for the Sho1 branch
k34 = 5	A coefficient for the input equation for the Sho1 branch (dimensionless)
k35 = 0.049 min^{-1}	Msb2active inactivation rate
k36 = 1 $(\mu M \cdot min)^{-1}$	Sho1 phosphorylation rate
k37 = 0.08 min^{-1}	Sho1p dephosphorylation rate
k38 = 1 $(\mu M \cdot min)^{-1}$	Ste11 phosphorylation rate
k39 = 0.06 min^{-1}	Ste11p dephosphorylation rate

Pbs2

$$\frac{d}{dt} Pbs2 = k20 \cdot Pbs2p - Ssk2p \cdot \frac{k18 \cdot Pbs2}{k19 + Pbs2} - Ste11p \cdot \frac{k40 \cdot Pbs2}{k41 + Pbs2} - Pbs2 \cdot V_r$$

$$\frac{d}{dt} Pbs2p = k23 \cdot Pbs2pp + Ssk2p \cdot \frac{k18 \cdot Pbs2}{k19 + Pbs2} + Ste11p \cdot \frac{k40 \cdot Pbs2}{k41 + Pbs2} - Ssk2p \cdot \frac{k21 \cdot Pbs2p}{k22 + Pbs2p}$$

$$-Ste11p \cdot \frac{k42 \cdot Pbs2p}{k43 + Pbs2p} - k20Pbs2p - Pbs2p \cdot V_r$$

$$\frac{d}{dt} Pbs2p = -k23 \cdot Pbs2pp + Ssk2p \cdot \frac{k21 \cdot Pbs2p}{k22 + Pbs2p} + Ste11p \cdot \frac{k42 \cdot Pbs2p}{k43 + Pbs2p} - -Pbs2p \cdot V_r$$

Concentrations: Pbs2 = 0.053 µM

k18 = 0.3080 min^{-1}	Maximal velocity of Pbs2p formation in the Sln1 branch
k19 = 0.001 µM	Michaelis constant of Pbs2p formation in the Sln1 branch
k20 = 0.11 min^{-1}	Pbs2p dephosphorylation rate
k21 = 2.655 min^{-1}	Maximal velocity of Pbs2pp formation in the Sln1 branch
k22 = 0.0005 µM	Michaelis constant of Pbs2pp formation in the Sln1 branch
k23 = 0.22 min^{-1}	Pbs2pp dephosphorylation rate

k40 = 0.08 min^{-1} Maximal velocity of Pbs2p formation in the Sho1 branch

k41 = 0.0001 μM Michaelis constant of Pbs2p formation in the Sho1 branch

k42 = 1.0296 min^{-1} Maximal velocity of Pbs2pp formation in the Sho1 branch

k43 = 0.0001 μM Michaelis constant of Pbs2pp formation in the Sho1 branch

Hog1

$$\frac{d}{dt}Hog1 = k26 \cdot Hog1p - Pbs2pp \cdot \frac{k24 \cdot Hog1}{k25 + Hog1} + k32 \cdot Hog1Nuclear - Hog1 \cdot V_r$$

$$\frac{d}{dt}Hog1p = Pbs2pp \cdot \left(\frac{k24 \cdot Hog1}{k25 + Hog1} - \frac{k27 \cdot Hog1p}{k28 + Hog1p}\right) - k26 \cdot Hog1p + k29 \cdot Hog1pp - Hog1pp \cdot V_r$$

$$\frac{d}{dt}Hog1pp = Pbs2pp \cdot \frac{k27 \cdot Hog1p}{k28 + Hog1p} - k29 \cdot Hog1pp - k30 \cdot Hog1pp - Hog1pp \cdot V_r$$

$$\frac{d}{dt}Hog1ppNuclear = k30 \cdot Hog1pp - k31 \cdot Hog1ppNuclear - Hog1ppNuclear \cdot V_r$$

$$\frac{d}{dt}Hog1Nuclear = k31 \cdot Hog1ppNuclear - k32 \cdot Hog1Nuclear - Hog1Nuclear \cdot V_r$$

Concentrations: Hog1 = 0.167 μM

k24 = 5.5368 min^{-1} Maximal velocity of Hog1p formation

k25 = 0.01 μM Michaelis constant of Hog1p formation

k26 = 0.1 min^{-1} Hog1p dephosphorylation rate

k27 = 5.5368 min^{-1} Maximal velocity of Hog1pp formation

k28 = 0.03 μM Michaelis constant of Hog1pp formation

k29 = 0.1 min^{-1} Hog1pp dephosphorylation rate

k30 = 0.3 min^{-1} Hog1pp import rate to nucleus

k31 = 0.9 μM Hog1ppNuclear dephosphorylation rate

k32 = 0.9 min^{-1} Hog1Nuclear export rate

Gpd1 Expression Module

$$\frac{d}{dt}Gpd1mRNA = k44 + k45 \cdot \frac{\left(\frac{Hog1ppNuclear \cdot Hot1}{k46}\right)^{k47}}{1 + \left(\frac{Hog1ppNuclear \cdot Hot1}{k46}\right)^{k47}} - k48 \cdot Gpd1mRNA - Gpd1mRNA \cdot V_r$$

$$\frac{d}{dt}Gpd1 = k49 \cdot Gpd1mRNA - k50 \cdot Gpd1 - Gpd1 \cdot V_r$$

Concentrations: Gpd1 mRNA = 0.00014 (rough estimation) Gpd1 = 0.0179 μM

k44 = 0.0001 min^{-1} Basal transcription level of Gpd1mRNA

k45 = 0.0014 min^{-1} Maximal rate of the formation of Gpd1mRNA

k46 = 0.0350 μM	Dissociation constant of the formation of Gpd1mRNA
k47 = 1.05	Hill coefficient for the formation of Gpd1mRNA
k48 = 0.7 min^{-1}	Gpd1mRNA degradation rate
k49 = 1 min^{-1}	Formation rate of Gpd1
k50 = 0.006 min^{-1}	Degradation rate of Gpd1

Glycerol and Biophysical Changes

$$\frac{d}{dt}Glycerol = k51 \cdot Gpd1 - k52 + k53 \cdot \frac{\left(\frac{1 - turgor(t)}{k54}\right)^{k55}}{1 + \left(\frac{1 - turgor(t)}{k54}\right)^{k55}} - Glycerol \cdot V_r$$

$$\frac{d}{dt}\,Volume = -G \cdot Lp \cdot (turgor - Ip + Ep)$$

$$Ep = Ep_{Steady\ state} + w \cdot NaCl$$ External pressure

$$turgor(t) = \begin{cases} turgor_{(t=0)} \cdot \frac{Volume(t) - Volume_{(turgor=0)}}{Volume_{(t=0)} - Volume_{(turgor=0)}} & if\ \ Volume(t) > Volume_{(turgor=0)} \\ 0 & else \end{cases}$$

$$Ip = \left(Os + 0.5 \cdot Glycerol \cdot (Volume + Vc)\right) \cdot 1^{-9} \cdot R \cdot T/Volume$$ Internal pressure

$$V_r = \frac{\frac{d}{dt}Volume}{(Volume + Vc)}$$ Volume ratio

Concentration: Glycerol = 600 mM

k51 = 7644 min^{-1}	Glycerol formation rate
k52 = 632.1237 min^{-1}	Glycerol outflow rate
k53 = 632.1237 min^{-1}	Maximal rate of channel closure.
k54 = 0.06 μM	Dissociation constant of channel closure
k55 = 0.54	Hill Coefficient of channel closure (dimensionless)
G = $72.4607 \cdot 10^{-12}\ m^2$	
Lp = $0.2497 \cdot 10^{-12}\ m^4 \cdot J^{-1} \cdot min^{-1}$	
w = $4.688 \cdot 10^6\ J \cdot m^{-3} \cdot M^{-1}$	
Os = $4176000 \cdot 10^{-9}$ µMol	Contribution of other osmolarity except glycerol
Vc = 23.2 fL	Uncompressible volume (not affected by osmotic changes)
R = $8.314 \cdot J \cdot K^{-1} \cdot M^{-1}$)	Gas constant
T = 303.15 K	Tempratur
NaCl = {0, 0.07, 0.1, 0.2, 0.4, 0.6, 0.8} M	Stress. 0 at steady state
Ep (steady state) = $0.6876 \cdot 10^6\ J \cdot m^{-3}$	Initial external pressure
turgor (t=0) = $0.875 \cdot 10^6\ J \cdot m^{-3}$	Initial turgor pressure
Volume (turgor=0) = 15.63 fL	compressible volume when turgor pressure = 0
Volume(t=0) = 34.8 fL	Initial compressible volume

EIGENSTÄNDIGKEITSERKLÄRUNG

Hiermit versichere ich, dass ich die vorliegende Masterarbeit erstmalig einreiche, selbständig
verfasst und keine anderen als die angegebenen Quellen und Hilfsmittel verwendet habe.

DECLARATION OF INDEPENDENCE

I hereby certify that I file the present master thesis for the first time, have written it independently and used no other sources and aids than those stated above.

Berlin, 27.01.2012

Gady Goldsobel